

Surfactant effect on nanoparticle formation by biphotonic reduction of silver ions in aqueous solution

著者	Umair Yaqub Qazi
学位授与機関	Tohoku University
学位授与番号	11301甲第16000号
URL	http://hdl.handle.net/10097/58851

博 士 論 文

**Surfactant effect on nanoparticle
formation by biphotonic reduction of
silver ions in aqueous solution**

(銀イオン水溶液の二光子還元によるナノ
粒子生成に及ぼす界面活性剤の効果)



Umair Yaqub Qazi

2014 年

Contents

Chapter 1: Introduction

1.1 Nanomaterial	2
1.2 Physicochemical properties and applications	2
1.3 Chemical synthesis and types of additives	5
1.4 Light mediated synthesis	8
1.5 Objective of this work	9
1.6 References	10

Chapter 2: Experimental

2.1 Chemical and additives	14
2.2 Experimental procedure and optical setup	16
2.3 Characterization techniques	17
2.3.1 Optical spectroscopy	17
2.3.2 Scanning electron microscopy (SEM)	18
2.3.3 Energy dispersive x-ray spectroscopy (EDX)	18
2.3.4 Dynamic light scattering (DLS)	19
2.4 References	23

Chapter 3: Surfactant free photo-synthesized silver nanocubes in aqueous solution of silver salt: effect of laser fluence and irradiation time

3.1 Abstract	25
3.2 Synthesis of AgNPs in aqueous solution of silver nitrate without using surfactants	26
3.3 Results and discussion	26
3.3.1 Optical properties	26

3.3.2 SEM analysis and EDX	29
3.3.3 Laser intensity dependence of AgNCs	31
3.3.4 Irradiation time dependence of AgNCs	33
3.3.5 Intensity effect on AgNCs	35
3.3.6 CW and pulsed UV light effect on initial process	36
3.3.7 Comparison of silver nitrate concentration	37
3.4 Effect of CW-UV light on growth process of AgNCs	38
3.4.1 Optical properties of NCs by CW light irradiation	39
3.4.2 SEM analysis of NCs after CW light irradiation	41
3.5 Conclusion	43
3.6 References	44
 Chapter 4: Effect of sodium dodecyl sulfate on the formation of silver nanoparticles by biphotonic reduction of silver nitrate in water	
4.1 Abstract	46
4.2 Introduction	47
4.3 Results and discussion	48
4.3.1 Comparison of photo-product by SEM and their size distribution	48
4.3.2 Optical properties	51
4.3.3 Estimation of molar absorption coefficient	53
4.3.4 Stoichiometry of photoreaction	55
4.3.5 Time profile of various SDS concentrations on growth process	58
4.3.6 Effect of sodium methyl sulfate (SMS)	59

4.3.7 Effect of SDS concentration on NPs formation	60
4.3.8 Role of SDS on growth process (Mechanism)	62
4.3.9 Concept of hemi-micelle formation	63
4.3.10 Number of SDS molecules required for single layer	65
4.4 Summary and Conclusion	66
4.5 References	67
Chapter 5: Effect of additives on photo-products	
5.1 Introduction	71
5.2 Results and discussion	71
5.2.1 Optical properties (Aerosol OT (AOT))	71
5.2.2 Time profile of AOT with various concentrations	75
5.2.3 Effect of AOT concentration on NPs formation process	77
5.2.4 Comparison between SDS and AOT	78
5.3 Sodium octyl sulfate (SOS)	79
5.3.1 Optical properties and SEM analysis	79
5.3.2 SOS concentration effect on NPs	82
5.4 Sodium hexyl sulfate (SHS)	83
5.4.1 Optical properties and SEM analysis	83
5.5 Sodium methyl sulfate (SMS)	86
5.5.1 Optical properties and SEM analysis	86
5.6 Hydrocarbon chain effect on AgNPs growth.	89
5.7 Effect of bis (p-sulfonate phenyl) phenyl phosphine dipotassium (BPPD)	90
5.7.1 Optical properties and SEM analysis	90

5.8 Conclusion	93
5.9 References	94
Chapter 6: Photochemical synthesis of AgNPs using UV pulsed laser irradiation in aqueous solution of silver acetate: effect of stabilizing agents	
6.1 Introduction	98
6.2 Results and discussion	98
6.2.1 Optical properties	98
6.2.2 Size, morphology and chemical composition	103
6.3 Conclusion	106
6.4 References	108
Chapter 7: Summary and conclusion	
7.1 Summary and conclusion	109

Acknowledgements

Chapter 1

Introduction

1 Introduction:

1.1 Nanomaterial

Nanotechnology has been the fastest growing area of manufacturing in the world and researchers have been interested in fabrication of new nanomaterial by adopting new and simple methods to make them. In the past few decades, there have been impressive achievements in the field of nanotechnology with numerous methodologies formulated to synthesize nanoparticles (NPs) of particular shape and size depending on specific requirements. A lot of attention is being given to develop clean synthesis methods to avoid use of toxic chemicals and synthesized materials for medical and pharmaceutical applications [1-2]. Nanometer sized metallic nanoparticles (NPs) are most sought materials because of their high dispersibility and easy attachment of moieties of choice at their high energy surfaces compared to other structures such as nanotubes. It has been demonstrated that preparation of nm sized NPs with homogeneous distribution can be conducted in aqueous solution using inexpensive and non-toxic surfactants such as glucose [3]. Among NPs, spherical geometry is most common [4-5] because of its natural occurrence. NPs of designated shape and size are also in demand as they fulfil specific requirements in electronics, medicine and pharmaceutical applications.

1.2 Physicochemical properties and applications

In general nanomaterials (NMs) have unique physicochemical properties compared to the bulk materials [6-8]. The optical and electronic characteristics of these nanomaterials effectively change their behavior in favor of potential applications [9-10] as photovoltaic devices, catalysts, semiconductors, and recently in medical diagnosis [11] and pharmaceutical products [12]. Silver (Ag) and gold (Au) NPs give plasmonic properties in visible region which make them potentially useful for electronic devices [13]. Ag NPs

have strong antimicrobial activities and have been used to prevent as well as to treat a wide variety of diseases [14-15]. Since physicochemical properties of NPs highly depend on their size and shape as shown in Figure 1.1 [16], the controlling shape and size of particles is important. It has been challenging to adopt a suitable method for synthesizing shape and size controlled metal nanoparticles [17]. Surface plasmon resonance has been used for many applications in various fields like medical, chemical, engineering, and environment protection. Plasmonic behavior of nanoparticles formed by using laser has attracted much attention especially using nanosecond (ns) Nd:YAG [18] and femtosecond (fs) Ti:Sapphire [19] lasers.














Shape	Illustration	LSPR ^a	Applications ^b	Method of Synthesis
Sphere and quasi-sphere		320 - 450	SERS; LSPR sensing; assembly	Polyol process (single-crystal); Citrate reduction (quasi-sphere)
Cube and truncated cube		400 - 480	SERS; LSPR sensing; assembly	Polyol process; Seed-mediated growth
Tetrahedron and truncated tetrahedron		350 - 450	SERS	Polyol process; Light-mediated Growth
Octahedron and truncated octahedron		400 - 500	Assembly	Polyol process; seed-mediated growth; light-mediated growth
Bar		350 - 900	SERS	Polyol process
Spheroid		350 - 900	SERS	Polyol process
Right bipyramid		500 - 700	-	Polyol process
Beam		-	Electron transport	Polyol process
Decahedron		350 - 450	-	Seed-mediated growth; light-mediated growth; citrate reduction
Wire and rod		380 - 460	Wave guiding; electronics; SERS; assembly	Seed-mediated growth
Polygonal plates and disc		350 - 1000	SERS; LSPR sensing	Light-mediated growth; polyol process
Branched structures		400 - 1100	SERS	Seed-mediated growth
Hollow structures		380 - 800	SERS; LSPR sensing	Template-directed growth

Figure 1.1 Over all view of the shapes, LSPR absorption peaks, demonstrated applications and methods for synthesis of silver (Ag) nanostructures [16]

1.3 Chemical synthesis and types of additives

Various methods have been used for synthesizing different nanoparticles; however, preparation of AgNPs is mainly done by reduction process using different salt precursors and a number of reducing agents such as sodium borohydride, dimethyl formamide, and hydrazine. In most of these methods toxic and hazardous chemicals are used, which may have potential environmental and biological implications [20-21]. Figure 1.2 shows a schematic diagram of various methods which have been adopted by researchers [22-26]. A variety of additives are also used along with these reducing agents which work as capping agents, stabilizing agents, dispersing agents like polymers, surfactants etc. as shown in Figure 1.3. These additives may have important roles to control the shape and size of synthesized products; however, it is very difficult to discuss the individual role of each.

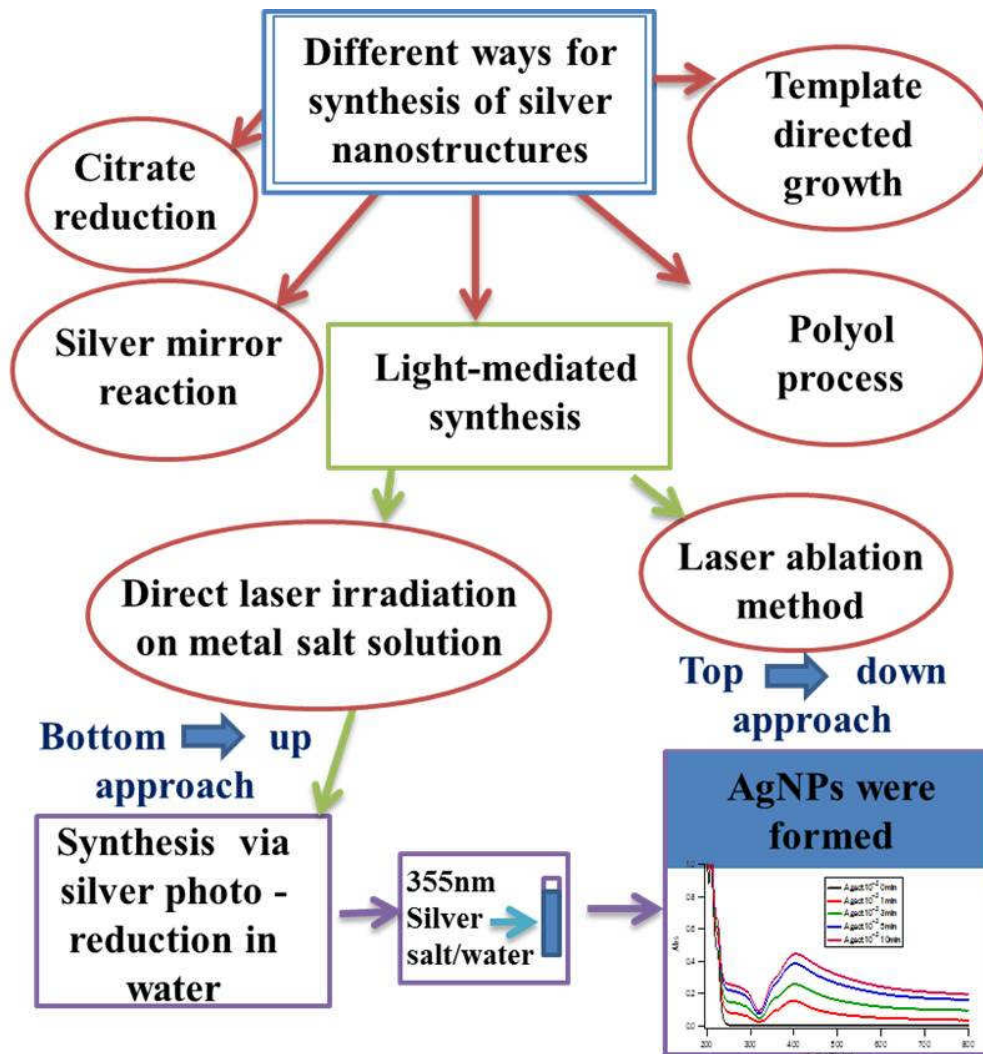
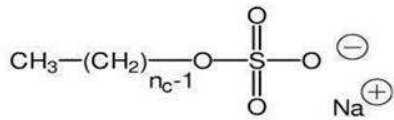


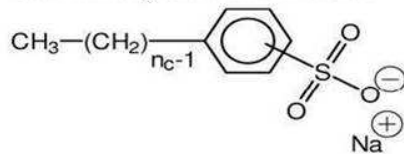
Figure 1.2 Flow chart diagram for various synthesis methods

Anionic

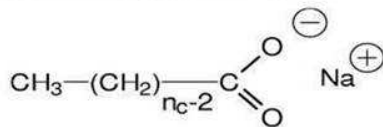
Sodium alkylsulfate



Sodium alkylbenzenesulfonate

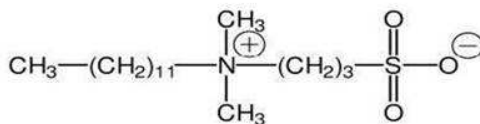


Sodium alkylcarboxylate

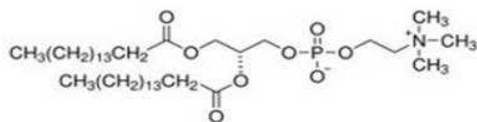


Zwitterionic

Alkyldimethylpropanesultaine

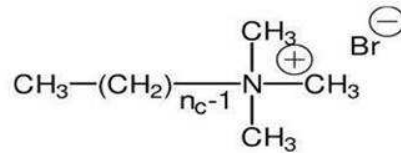


Dipalmitoylphosphatidylcholine

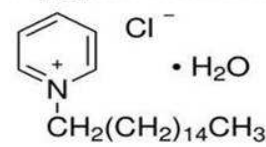


Cationic

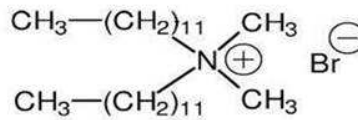
Alkyltrimethylammonium bromide



Cetylpyridinium chloride

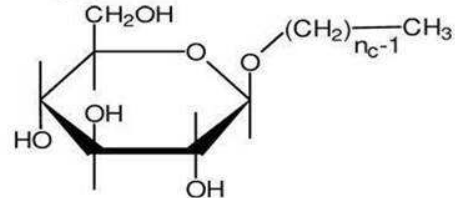


Dialkyldimethylammonium bromide



Nonionic

Alkylglucosides



Poly(ethylene oxide)
iso-octylphenyl ether

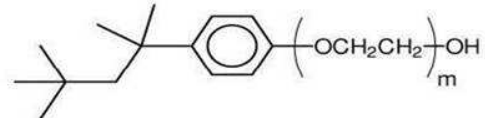


Figure 1.3 Chemical structures of common surfactants

1.4 Light mediated synthesis

In recent years, researchers have much interest in developing environmental friendly methods for nanoparticle synthesis to remove toxic chemicals. NPs synthesized by laser ablation are taking a center stage due to its high NPs purity and benign environmental effects. When a solid target immersed in a solution and irradiated with laser, radiation energy is absorbed by the material and the ejection of atoms/small atomic clusters takes place [27-29]. This method has been used to synthesize AgNPs in solution without using chemicals except for a dispersing agent [27]; however, it forms particles with large size distribution through a fast coalescence and agglomeration of ablated species [30]. After the formation of large size particles in a solution, additional laser irradiation is effective to reshape and resize the large particles through melting and fragmentation process [31]. It is also difficult to control the shape of synthesized product. In this method selection of suitable surface active dispersing agent is important to make a stable colloidal solution [32-33].

There is another photochemical reduction method for synthesizing NPs and limited studies have been reported which may be similar to those in radiolysis rather than laser ablation to yield various fragments. In this method laser light is used as a reducing agent and prepared stable NPs in an aqueous solution of metal salts containing suitable dispersing agents [34-35]. It also enables us to produce metal NPs with narrow size distribution which is completely free from extra reducing chemicals and we can investigate the individual role of each additive.

1.5 Objectives of thesis

Our main objectives of this thesis are

1. Utilize UV irradiation for reducing silver salts in aqueous solution and fabricate uniform silver nanoparticles (AgNPs) using possible fewer additives.
2. Examine the individual role of surfactants on the regulation of NPs in synthesis process.
3. Discuss the effect of surfactants on the growth process of NPs in a wide range of concentrations.
4. Understanding mechanism of AgNPs growth by studying the surface chemistry on the formation of hemi-micelle (HM) structures.

1.6 References

- [1] Z. Aguilar, *Nanomaterials for Medical Applications*, Elsevier, **2012**.
- [2] M. Ferrari, *Nature Reviews* **2005**, 5, 161.
- [3] S. Panigrahi, S. Kundu, S. K. Ghosh, S. Nath, T. Pal, *J. Nanopart. Res.* **2004**, 6, 411.
- [4] F. Mafune, J. Kohno, Y. Takeda, T. Kondow, H. Sawabe, *J. Phys. Chem. B* **2000**, 104, 9111.
- [5] A. Pyatenko, K. Shimokawa, M. Yamaguchi, O. Nishimura, M. Suzuki. *Appl. Phys. A* **2004**, 79, 803.
- [6] G. Schmid, *Chem. Rev.* **1992**, 92, 1709.
- [7] M. P. Pileni, *Langmuir* **1997**, 13, 3266.
- [8] A. Henglein, *Chem. Rev.* **1989**, 89, 1861.
- [9] Al. Linsebigler, G. Lu, J. T. Yates, *Chem. Rev.* **1995**, 95, 735.
- [10] M. A. Fox, M. T. Dulay, *Chem. Rev.* **1993**, 93, 341.
- [11] L. Wang, X. Gan, *Microchim. Acta.* **2009**, 164, 231.
- [12] F. Lince, D. L. Marchisio, A. A. Barresi, *Chem. Eng. Res. Des.* **2009**, 87,543.
- [13] Y. K. Seo, S. Kumar, G. H. Kim, *J. Nanosci. Nanotechnol.* **2011**, 11(6), 4852.
- [14] L. Ming, *Med. Res. Rev.* **2003**, 23, 697.
- [15] T.C. Chuang, Y.C. Liu, C.C. Wang, *J. Raman Spectrosc.* **2005**, 36, 704.
- [16] M. Rycenga, C. M. Cobley, J. Zeng, W. Li, C. H. Moran, Q. Zhang, D. Qin, Y. Xia, *Chem. Rev.* **2011**, 111, 3669.
- [17] C. H. Bae, S. H. Nam, S. M. Park, *Appl. Surf. Sci.* **2002**, 197–198, 628.
- [18] T. Tsuji, K. Iryo, Y. Nishimura, M. Tsuji, *J. Photochem. Photobiol. A, Chem.* **2001**, 145, 201.

- [19] H. Zeng, C. Zhao, J. Qiu, Y. Yang, G. Chen, *J. Cryst. Growth.* **2007**, *300*, 519.
- [20] P. Seuta, A. Chakarborty, D. Seth, M. U. Bhatta, P. V. Satyam, N. Sarka, *J. Phys. Chem.C* **2007**, *11*, 3901.
- [21] I. M. Ramirez, S. Bashir, Z. Luo, J. L. Liu, *Colloids Surf. Biointerfaces.* **2009**, *73*, 185.
- [22] A. L. Pyayt, B. J. Wiley, Y. Xia, A. Chen, L. Dalton, *Nature Nanotechnol.* **2008**, *3*, 660.
- [23] M. Rang, A. C. Jones, F. Zhou, Y. Z. Li, B. J. Wiley, Y. Xia, M. B. Raschke, *Nano Lett.* **2008**, *8*, 3357.
- [24] I. Yoon, T. Kang, W. Choi, J. Kim, Y. Yoo, W. S. Joo, H. Q. Park, H. Ihee, J. B. Kim, *J. Am. Chem. Soc.* **2009**, *131*, 758.
- [25] Q. Zhang, W. Li, L. P. Wen, J. Chen, Y. Xia, *Chem-Eur. J.* **2010**, *132*, 11372.
- [26] A. L. Koh, K. Ba0, I. Khan, W. E. Smith, G. Kothleitner, P. Nordlander, S. A. Maier, W. D. McComb, *ACS Nano.* **2009**, *3*, 3015.
- [27] T. Tsuji, D. H. Thang, Y. Okazaki, M. Nakanishi, Y. Tsuboi, M. Tsuji, *Appl. Surf. Sci.* **2008**, *254*, 5224.
- [28] R. A. Ganeev, M. Baba, A. I. Ryasnyansky, M. Suzuki, H. Kuroda, *Opt. Commun.* **2004**, *240*, 437.
- [29] M. A. Sobhan, M. Ams, M. J. Withford, E. M. Goldys, *J. Nanopart. Res.* **2010**, *12*, 2831.
- [30] S. Besner, A. V. Kabashin, M. Meunier, *Appl. Phys. A* **2007**, *88*, 269.
- [31] F. Mafune, J. Kohno, Y. Takeda, T. Kondow, *J. Phys. Chem. B* **2001**, *105*, 9050.
- [32] J. Chandradassa, M. Balasubramanianb, D. S. Baec, J. Kimd, K. H. Kima, *J.*

Alloys Compd. **2010**, 491, L25.

[33] F. Mafune, J. Kohno, Y. Takeda, T. Kondow, *J. Phys. Chem. B* **2002**, 106, 7575.

[34] T. Nakamura, K. Takasaki, A. Ito, S. Sato, *Appl. Surf. Sci.* **2009**, 255, 9630.

[35] J. P. Abid, A. W. Wark, P. F. Brevet, H. H. Girault, *Chem. Commun.* **2002**, 792.

Chapter 2

Experimental

2 Experimental

In this chapter, experimental procedure, all kind of chemicals as well as the characteristic techniques are discussed in detail.

2.1 Chemical and additives

Silver salts precursors; silver nitrate (AgNO_3 , 99.9%) and silver acetate (CH_3COOAg , 99.00 % pure) were purchased from Wako pure Chemical industries, Ltd. and Sigma-Aldrich Company respectively and used without further purification. A variety of additives were being used to know their effect on the formation process of silver nanoparticles as follow:

- Sodium dodecyl sulphate (SDS, Wako pure Chemicals, Co.)
- Sodium bis(2-ethyl hexyl) sulfosuccinate (AOT, Wako pure Chemicals, Co.)
- Cetyl trimethyl ammonium bromide (CTAB, Wako pure Chemicals, Co.)
- Bis(p-sulfonatophenyl) phenylphosphine dihydrate dipotassium salt (BPPD, Wako pure Chemicals, Co.)
- Sodium methyl sulfate (SMS, Tokyo Chemical Industry, Co. Ltd)
- Sodium hexyl sulfate (SHS, Wako pure Chemicals, Co.)
- Sodium octyl sulfate (SOS, MP Biomedicals, LLC, France.)

There chemical structures are presented in Figure 2.1

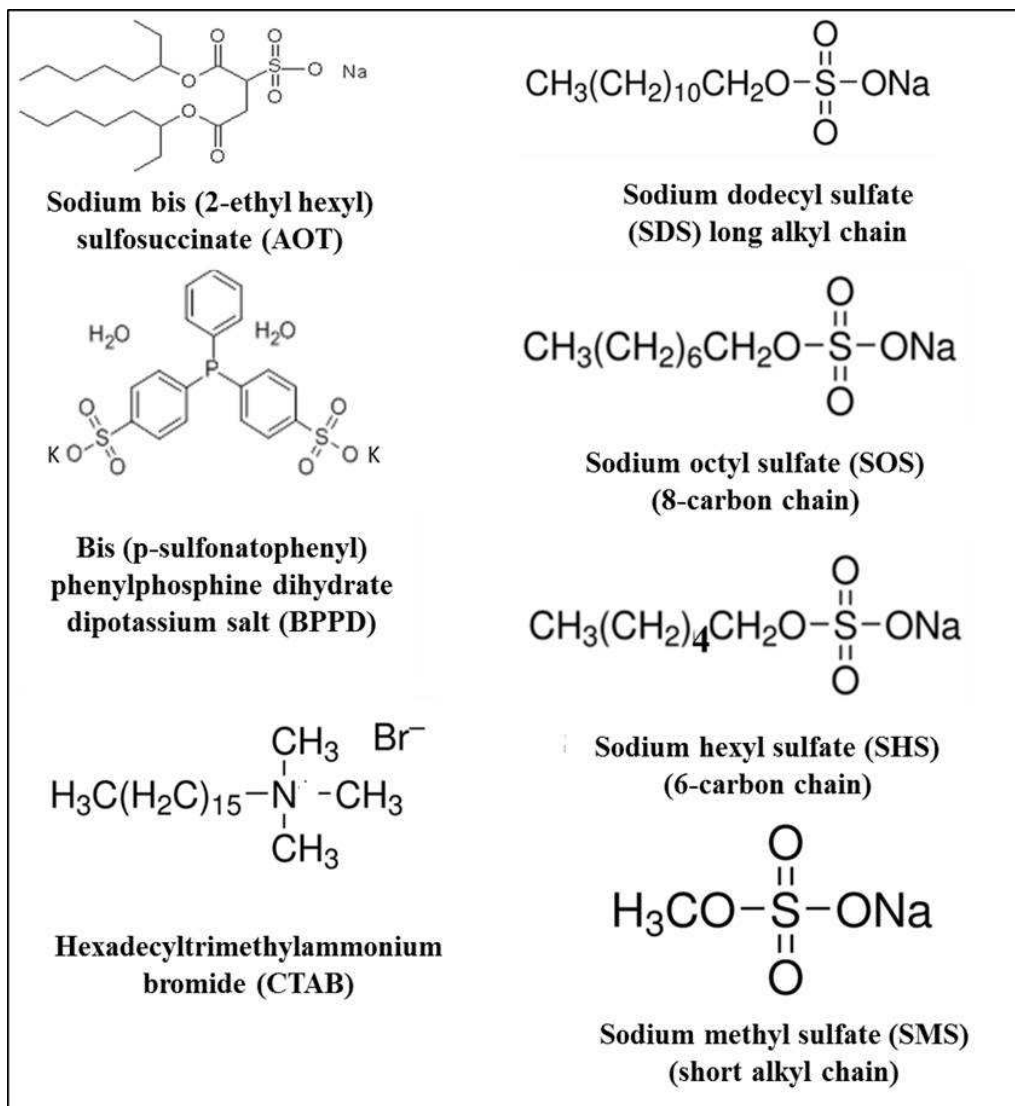


Figure 2.1 Structural formulas of chemicals used in this study

2.2 Experimental procedure and optical setup

Aqueous solutions of silver salt (Ag - salt) with various concentrations were prepared by dissolving silver salt precursors; silver nitrate and silver acetate in water with and without using additives. A sample solution was transparent at certain concentration before pulsed laser irradiation. A quartz cell, ($10 \times 10 \times 45 \text{ mm}^3$) optically transparent at laser wavelength 355 nm was used as a sample holder. Laser intensity was controlled with voltage controller and nanosecond (ns) laser pulses were generated by a UV laser (Quantel, Brilliant, wavelength: 355 nm; pulse width: 6 ns; repetition rate: 10 Hz) to synthesize nanoparticles. The volume of sample solution in a quartz cell was kept 3 ml for all experiments. The cell holder was placed on a magnetic stirring plate for controlled convection of the solution and the laser beam was directly introduced to the sample solution without using focus lens. The spot size diameter of laser beam was 4.6 mm. Figure 2.2 shows a schematic diagram of the

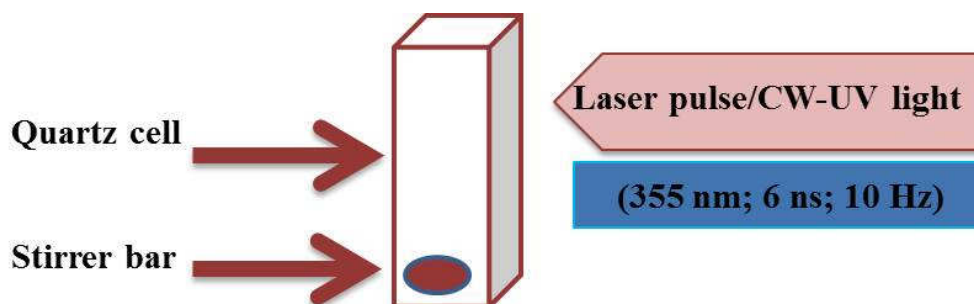


Figure 2.2 Experimental arrangements for NP synthesis

experimental setup. All experiments were performed at 25°C and 1 atm pressure. To know the effect of CW-UV light on aqueous solution of Ag salts and prepared colloidal solutions, we use a CW-UV light source (Lightening Cure LC8, Hamamatsu). CW-UV light was passed through a band pass filter (348 nm ± 5 nm, 3 mW) for comparison with ns laser wavelength.

2.3 Characterization techniques

2.3.1 Optical Spectroscopy

Optical spectroscopy has been widely used for the characterization of nanomaterials. UV-Vis spectroscopy measures the absorption of light due to its interaction with sample molecules. The metal nanoparticles exhibit an intense absorption band in the ultraviolet-visible region, known as the surface plasmon absorption band (SPAB) [1-7]. This technique measures the intensity of light passing through a sample (I), and compares it to the intensity of light before it passes through the sample (I_0). ϵ is the molar absorptivity coefficient, b is the path length, and c is the concentration. The method is most often used in a quantitative way to determine concentrations of an absorbing species in solution, using the Beer-Lambert law:

$$A(\lambda) = -\log(\%T) = \epsilon \times b \times c \quad (1)$$

The photochemical reduction of silver salt to silver metal was monitored visually and

by recording the UV-visible spectra of the preparations is one of the most widely used technique for characterization of NPs [8]. The appearance of plasmon resonance band indicating the characteristic of NPs formation. UV-visible extinction spectra of synthesised Ag metal colloidal solutions were recorded using UV-visible spectrophotometer (Shimadzu UV-1600 PC).

2.3.2 Scanning electron microscopy (SEM)

Electron microscopy is a commonly used tool to determine morphology and size distribution of nanoparticles. It is a type of electron microscope that provides the information about the sample structure and composition by scanning of focused beam of electrons. For this purpose, a small portion of the solution with photoproducts was drop-cast and dried on ITO substrates in a desiccator and used scanning electron microscopy (SEM, Hitachi, FE-SEM-S4300, 15.0 kV) for structural characterization of AgNPs formed in the solution.

2.3.3 Energy dispersive x-ray spectroscopy (EDX)

It is an analytical technique used for the elemental analysis or chemical characterization of a sample used in association with scanning electron microscopy (SEM). During SEM measurements, a sample is placed in a vacuum and irradiated with accelerated electrons. The electron beam excites the sample and produces

x-rays to release excess energy. This x-rays energy is the characteristic of corresponding atoms and observed in the form of peaks in the spectrum.

2.3.4 Dynamic light scattering (DLS)

Dynamic light scattering (DLS) is also known as photon correlation spectroscopy (PCS), which provides the information on the size and polydispersity of the particles. The particles in a solution have Brownian motion due to their constant motion, the intensity of light scattered by the particles with time dependent fluctuations. The analysis of intensity fluctuations helps to determine the diffusion coefficient D . Once the diffusion coefficient is established, the hydrodynamic radius of the particles can be derived via the Stokes-Einstein equation:

$$R_H = \frac{k_B T}{6\pi\eta_0 D} \quad (2)$$

Where R_H is the hydrodynamic radius, i.e., the radius of the sphere that diffuses at the same speed as the given particle, k_B is the Boltzmann constant, T is the absolute temperature, and η_0 is the suspension viscosity.

The measured particle size is related to the correlation function, which defines the degree of similarity between two signals over a period of time [9]. The autocorrelation function $C(\tau)$ can be defined as follows:

$$C(\tau) = \langle I(t)I(t+\tau) \rangle \quad (3)$$

Where $I(t)$ is the signal intensity measured at a given time and $I(t + \tau)$ is the signal intensity measured after a time delay τ . A perfect correlation coming from comparison of signal intensity at (t) with itself is reported as 1. In the case of a monodisperse suspension of spheres, the autocorrelation function can be treated as exponential decay

$$C(\tau) = \exp(-T\tau) \quad (4)$$

Where T is the decay rate related to the diffusion coefficient by the formula

$$T = Q^2 D \quad (5)$$

in which Q is the length of the scattering vector defined as

$$Q = \frac{4\pi n}{\lambda} \sin \frac{\theta}{2}. \quad (6)$$

Here, the refractive index is denoted by n and θ is the angle between the sample and the detector. As shown in Figure 2.3 the rate of decay for the correlation function is related to the particle size. Since large particles move slowly, the intensity of scattering also fluctuates slowly and the rate of decay is much slower than for quickly moving, smaller particles.

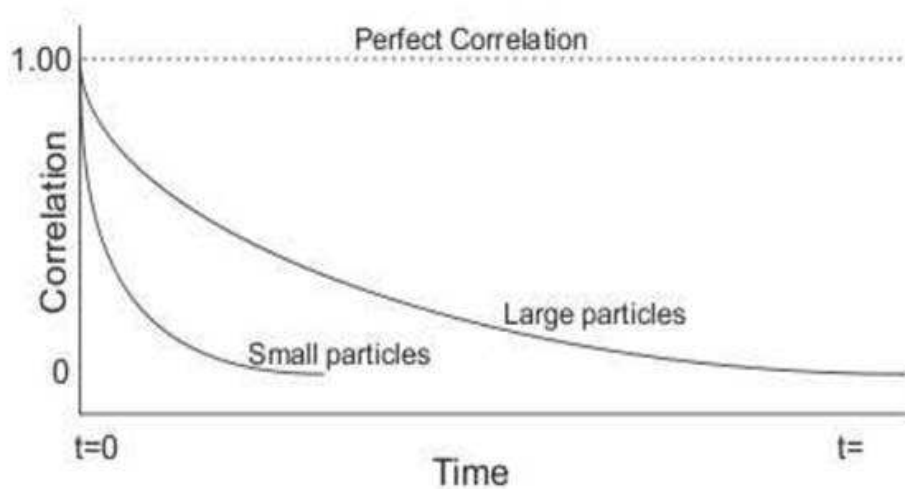


Figure 2.3 Correlation function vs time for small and large particles [10]

Once the correlation function has been measured, the decay rates can be extracted for a number of size classes to calculate the size distribution of a sample [10]. Figure 2.4 presents a typical size distribution graph.

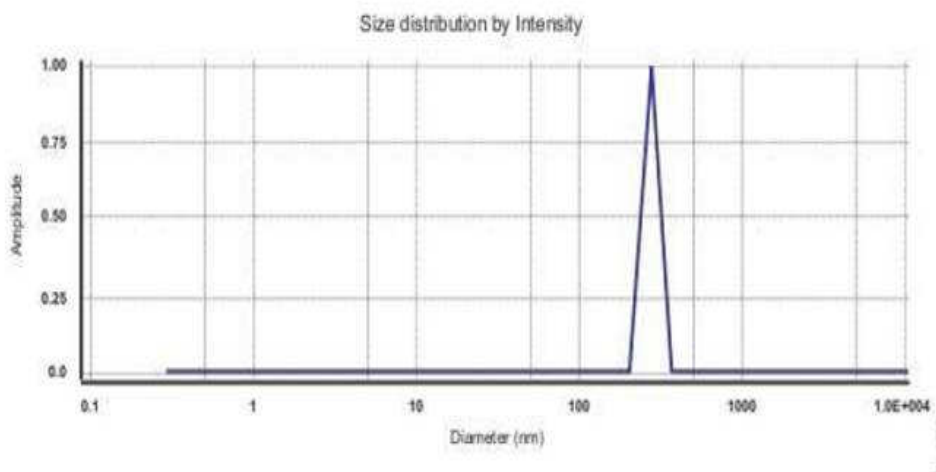


Figure 2.4 Typical size distributions by intensity graph [10]

The x axis shows the size distribution and the y axis shows the relative intensity of scattered light.

A typical DLS measuring system is shown in Figure 2.5 a laser light, being a source of monochromatic and coherent light illuminates the sample within the cell. Most of the laser beam passes straight through the solution and detector measures the intensity of the scattered light. An attenuator is used to control the intensity of the laser. The scattering light is passed to a correlator, which compares its intensity at time intervals to derive the rate

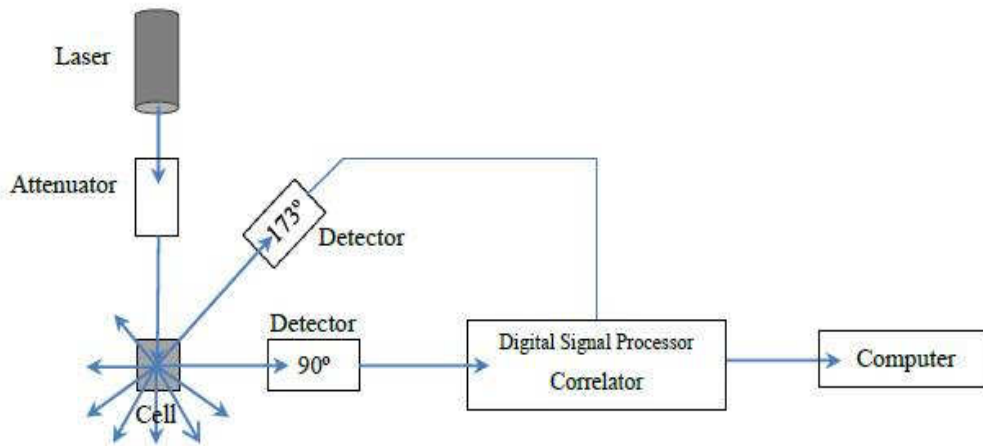


Figure 2.5 Optical configurations of the Malvern instruments for dynamic light scattering measurements

at which the intensity is changing. The resulting information is passed to a computer, ready for analysis. All the measurements were performed at 25°C. The presented size values are an average from at least three subsequent runs with ten measurements.

2.4 References

- [1] J. P. Wilcoxon, J. E. Martin, P. Provencio, *J. Chem. Phys.* **2001**, *115*(2), 998.
- [2] M. Zheng, M. Gu, Y. Jin, G. Jin, *Mater. Res. Bull.* **2001**, *36*, 853.
- [3] W. C. Bell, M. L. Myrick, *J. Colloid Interf. Sci.* **2001**, *242*, 300.
- [4] W. Cai, H. Hofmeister, T. Rainer, *Physica. E* **2001**, *11*, 339.
- [5] G. Schider, J. R. Krenn, W. Gotschy, B. Lamprecht, H. Ditlbacher, A. Leitner, *J. Appl. Phys.* **2001**, *90*, 3825.
- [6] J. J. Mock, M. Barbic, D. R. Smith, D. A. Schultz, S. Schultz, *J. Chem. Phys.* **2002**, *116*, 6755.
- [7] Y. Liu, C. Liu, L. Chen, Z. Zhang, *J. Colloid Interf. Sci.* **2003**, *257*, 188.
- [8] P. Y. Sun, P. Atorngitjawat, M. J. Meziani, *Langmuir* **2001**, *17*, 5707.
- [9] W. Sch[´]artl, *Light Scattering from Polymer Solutions and Nanoparticle Dispersion*. Springer-Verlag, **2007**.
- [10] *Zetasizer NanoSeries User Manual*, Malvern Instruments Ltd. Worcestershire, UK. **2003**.

Chapter 3

Surfactant free photo-synthesized silver nanocubes in an aqueous solution of silver nitrate: effect of laser fluence and irradiation time

3.1 Abstract

Silver nanocubes (AgNCs) were fabricated by ultraviolet (UV) nanosecond (ns) pulse laser irradiation in aqueous solution of silver salt in the absence of reducing agents. After laser irradiation, a broad absorption peak was observed at 405 nm due to the formation of silver nanoparticles (AgNPs) in a solution. The detailed characterization of photochemically synthesized product was done by means of a UV/Vis. spectroscopy and scanning electron microscope (SEM). SEM images showed that nanocubes (NCs) with an average size range of 75 – 200 nm were fabricated after 10 min laser irradiation. Effect of laser intensity and UV irradiation time were also investigated which had significant impact on size and shape of NCs. The slope value 1.5 implies that initially, it was a two photon process and later turned into a single photon process. CW-UV light experimental results also support our hypothesis that the growth process of AgNCs was done by single photon absorption and increased their size.

3.2 Synthesis of AgNPs in aqueous solution of silver nitrate without using surfactants.

In this chapter, I described the formation of AgNPs in the absence of surfactants. AgNPs were synthesized by irradiating 355 nm pulsed laser light as discussed in experimental section. Sample solutions of various concentrations (0.2 and 1 mM) were prepared by dissolving silver nitrate in ultra-pure water.

3.3 Results and discussion

3.3.1 Optical properties

The optical properties of metal nanoparticles are highly dependent on their size and shape [1-4]. Prepared silver salt solution did not show optical absorption at 355 nm nor in the visible region; however, when the sample solution was irradiated with nanosecond UV laser pulses, a new broad absorption peak observed at around 405 nm due to the surface plasmon resonance (SPR) of photo-chemically synthesized AgNPs as shown in Figure 3.1 [5]. The absorption peak around 302 nm is due to the presence of nitrate ions in the solution [6]. Figure 3.1a, corresponds with various laser intensities after 10 min irradiation time while Figure 3.1b, corresponds with various irradiation times at high laser intensity (290 mJ/cm^2). Broadening of the peak towards the longer wavelength in Figure 3.1a, 1b, is due to the formation of wide range size

distribution of AgNPs in the solution and their aggregates. As shown in Figure 3.1a, the absorbance of products increased with the intensity of laser implying that the number of products increased with laser intensity. It was also noticed that the peak shift from 415 nm to 405 nm with longer irradiation time along with the broadening in spectra towards the longer wavelength. Red shift corresponds with size reduction and broadening in spectra corresponds with growth in size or aggregation. The position and shape of the plasmon absorption band of noble metal nanoparticles is strongly dependant on their shape, dielectric medium and surface absorbed species [7-8]. Figure 3.1c shows absorption spectra observed after CW-UV light (358 nm) irradiation at various times. There was no clear absorption peak observed as compared to the absorption spectra obtained after ns laser irradiation. Based on calculation, we need 167 min. irradiation time for CW-UV light to achieve photon energy equal to 1 minute ns pulse laser energy.

We concluded from the experimental result that CW-UV light did not have enough energy to initiate the reaction. However, in case of ns laser experiment, AgNPs were obtained as a result of photo reduction of silver ions present in an aqueous solution.

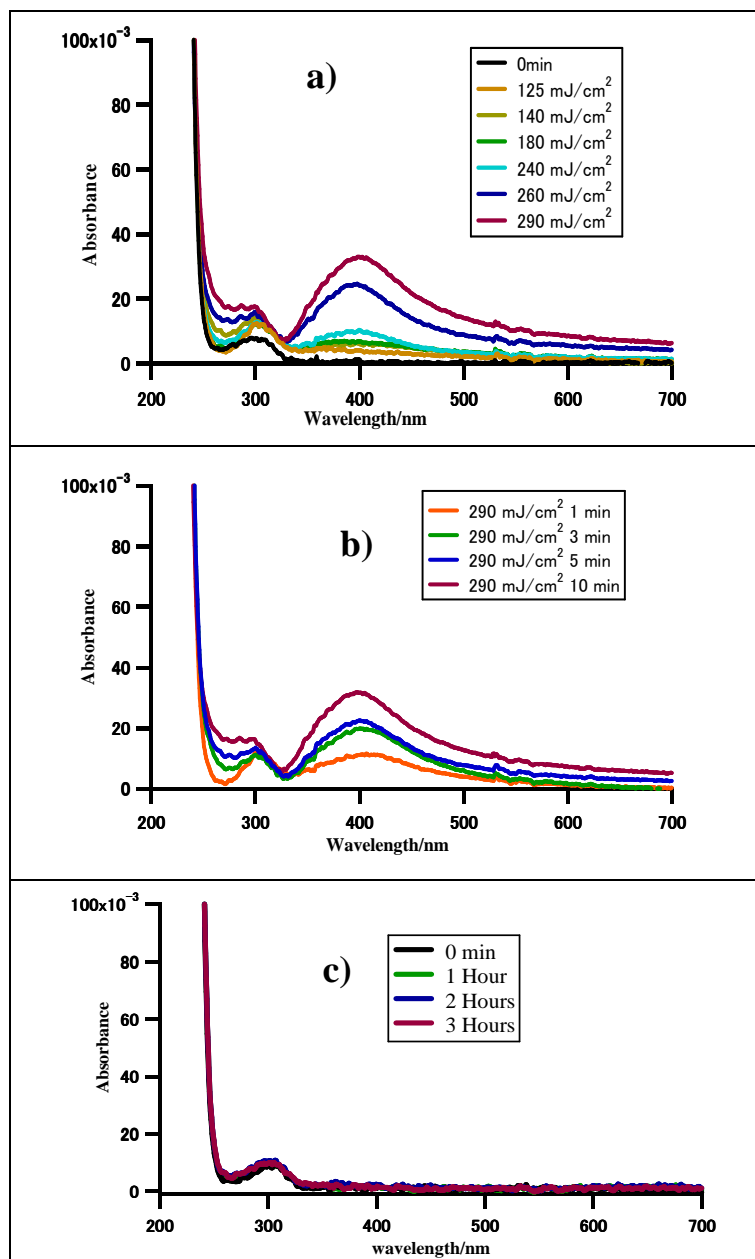


Figure 3.1 (a) Absorption spectra observed after 10 min irradiation at various laser intensities. (b) Absorption spectra observed after various irradiation time at high laser intensity (290 mJ/cm²). (c) Absorption spectra observed after CW-UV light (358 nm) irradiation at various times.

3.3.2 SEM analysis and EDX

Silver nanostructures were formed as a result of photo-reduction of Ag^+ ions present in a solution and confirmed with images obtained by SEM as shown in Figure 3.2. A series of experiments were performed by varying parameters such as irradiation time and laser intensity. The synthesized photo-product had a broad size and shape distribution along with the formation of cubic, irregular and spherical AgNPs. Small size (< 30 nm) silver nanoparticles are not visible in SEM images due to the limitation of the instrument. Among others, it was observed that the size of AgNCs increased with the laser intensity and the irradiation time. These results were also comparable with the UV-visible spectra of the solution which showed the spectral broadening due to the scattering from large size particles or aggregates present in the solution [9]. The elemental analysis of AgNPs was performed using an energy-dispersive X-ray (EDX) spectrometer on the SEM. as shown in Figure 3.3.

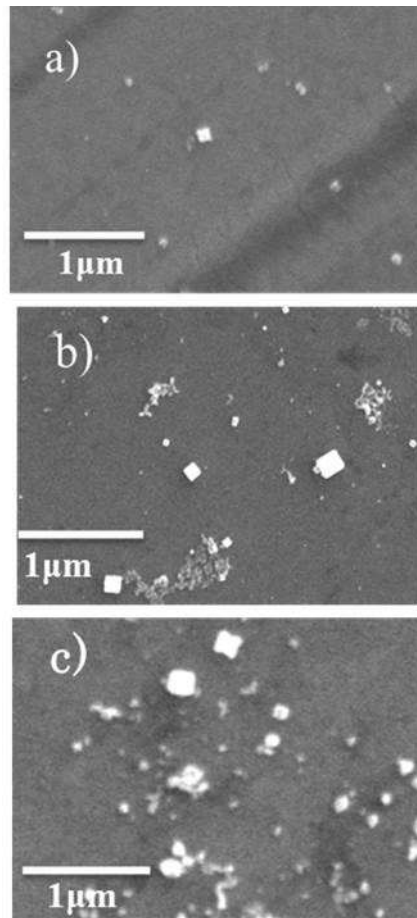


Figure 3.2 SEM images of silver nanostructures, synthesized by laser Irradiation, in an aqueous solution of silver nitrate. It confirms the presence of large size AgNCs which increased their size with an increase in laser intensity. However, at high intensity round shape silver particles were also formed. Images obtained at various intensities after 10 min irradiation were [a] lower intensity ($125 - 140 \text{ mJ/cm}^2$) [b] middle intensity ($180 - 240 \text{ mJ/cm}^2$) [c] Higher intensity ($260 - 290 \text{ mJ/cm}^2$).

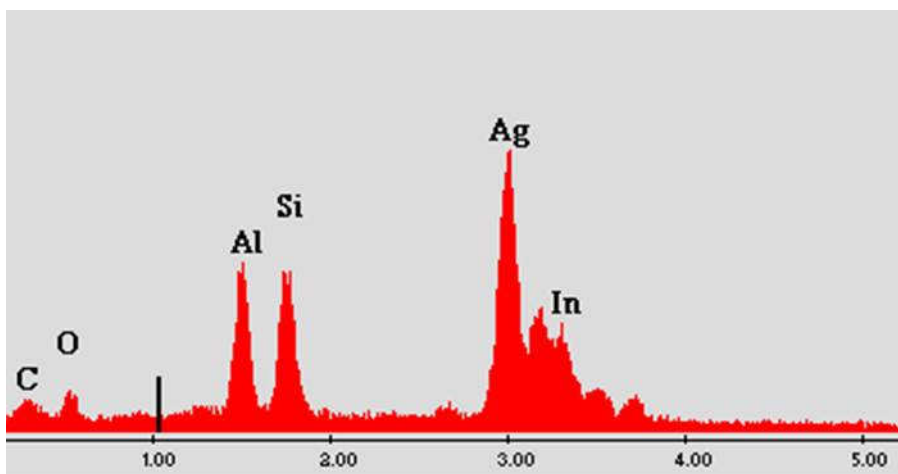


Figure 3.3 EDX spectrum of prepared silver nanoparticles. Other elemental peaks were observed due to the preparation of sample on Indium Titanium Oxide (ITO).

3.3.3 Laser intensity dependence of AgNCs

The size and shape of AgNCs was highly depended on laser intensity, as shown in Figure 3.4. It shows that the size distribution of AgNCs obtained after 10 min irradiation with different laser intensities. The results can be divided into three categories on the bases of laser intensity i.e, [i (a, b)] high intensity (260 – 290 mJ/cm^2), [ii (c, d)] middle intensity (180 - 240 mJ/cm^2) and [iii (e, f)] lower intensity (125 - 140 mJ/cm^2) respectively. At middle laser intensity, the average size of AgNCs was 75 and 100 nm, which increased to 175 and 200 nm at high laser intensity (290 mJ/cm^2) while, at low intensity (125 - 140 mJ/cm^2) few number of AgNCs were

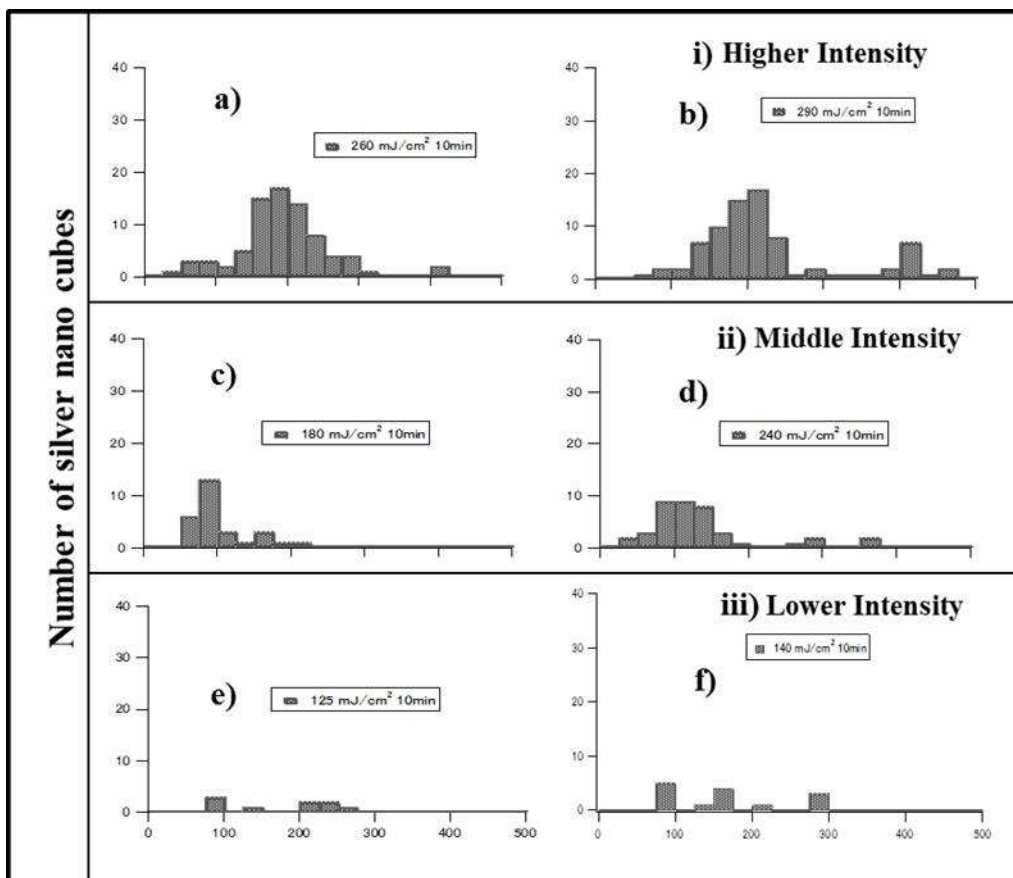


Figure 3.4 Size distribution of silver AgNCs after 10 min irradiation at higher [i (a, b)] (260 & 290 mJ/cm²), [ii (c, d)] middle (180 & 240 mJ/cm²) and lower intensity [iii (e, f)] (125 & 140 mJ/cm²). The size of AgNCs is highly dependent on laser intensity as size increases with an increase in laser intensity

observed and there was no clear indication of the specific size distribution of AgNCs.

These results imply that the size of AgNCs increased with an increase in laser intensity.

The growth process of AgNCs can be explained as; however, the exact mechanism is not confirmed. Ag ions accept an electron and go to the zero state of silver. This process starts as the irradiation start. As the number of particles increases in the solution, NCs may absorb 355 nm light and grow in sizes.

3.3.4 Irradiation time dependence of AgNCs

Figure 3.5 shows the laser irradiation time dependence of size distribution of AgNCs with high laser intensity. The results clearly show that irradiation time also had great impact on the size of AgNCs. In a short time, (< 5 min) with high laser intensity (290 mJ/cm²), less than 100 nm sized AgNCs were produced. However, large sized AgNCs were not observed at this stage. As the time increased up to 10 min., large sized (200 nm) AgNCs were formed. According to these results, the growth process of AgNCs with irradiation time could be explained. As will be discussed later, Ag⁺ ions accept electron and go to the neutral state of Ag upon laser irradiation. At the beginning of the reaction, the process of converting Ag⁺ ions into Ag particles was dominant to make Ag colloidal solution. There is a chance for aggregation as we did not use any dispersing agents. Another possibility is to absorb 355 nm laser light by the synthesized product which can be used to reshape AgNPs to form an observed specific shape that is known as the tailoring effect of laser light [10].

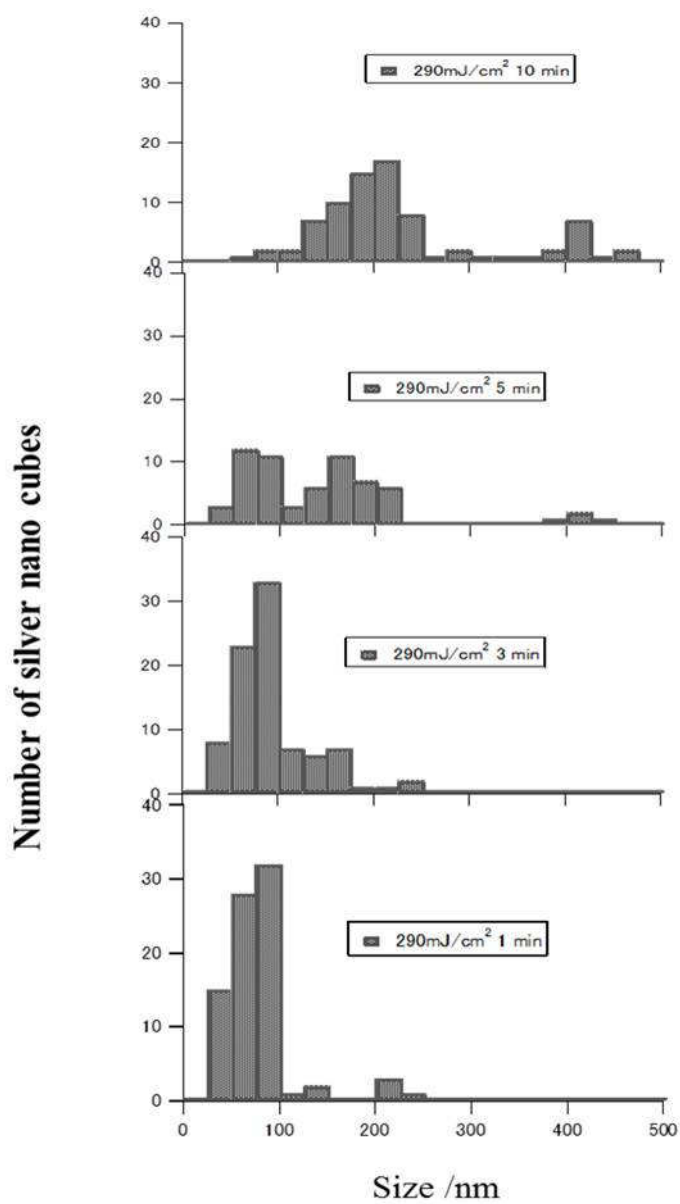


Figure 3.5 Size distribution of AgNCs synthesized with 290 mJ/cm² after different irradiation time. Small sized AgNCs are formed first (short time) which increases their size with an increase in irradiation time. (Growth process of AgNCs) These results are

also corresponding with laser intensity data.

3.3.5 Intensity effect on AgNCs

Figure 3.6 shows the laser intensity dependence of numbers of AgNCs. Several SEM images were taken to determine the number of AgNCs. Ten SEM images were used for all laser intensities to count the number of AgNCs. All parameters were kept same for all SEM images. The plot shows that the numbers of AgNCs increased with an increase of the laser intensity. The inset is a log-log plot after 1 min irradiation, which gave a slope value 1.5. This value indicates that, this is not a simple single photon process. On the bases of slope value, we may conclude that initially it is a biphotonic process. Photoproducts synthesized with former pulses may absorb a UV pulse and be excited resulting in growth in AgNCs. For the investigation of NCs formation, a CW light source was used to confirm the growth mechanism.

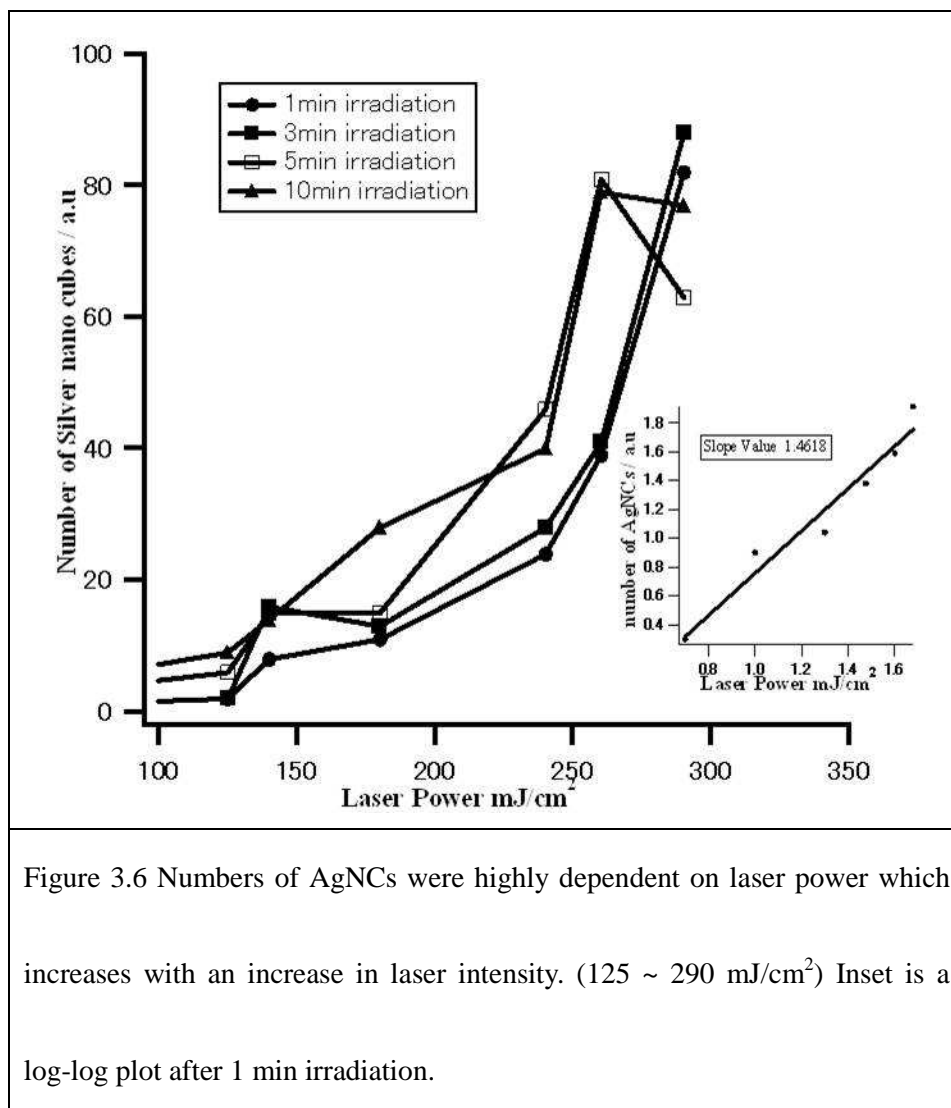


Figure 3.6 Numbers of AgNCs were highly dependent on laser power which increases with an increase in laser intensity. (125 ~ 290 mJ/cm²) Inset is a log-log plot after 1 min irradiation.

3.3.6 CW and pulsed UV light effect on initial process

Comparison between CW and pulsed UV light irradiation helps us to know about the starting point of the process. In the case of pulsed laser irradiation, an absorption band appears around at 405 nm which confirmed the formation of AgNPs. However, CW-UV light did not effect on a sample solution even irradiated for 3 hours, although

the total irradiation energy was kept same as in the case of pulsed laser irradiation for 1 min [see Figure 3.1 (a, c)]. These results imply that it is not a simple single photon process.

3.3.7 Comparison of silver nitrate concentration

Sample solutions having different concentrations (0.2 mM and 1 mM) were prepared by dissolving silver nitrate in ultra pure water and irradiated with 355 nm nanosecond pulse laser light at high intensity (300 mJ/cm^2 pulse). Different absorption spectra were observed as shown in Figure 3.7.

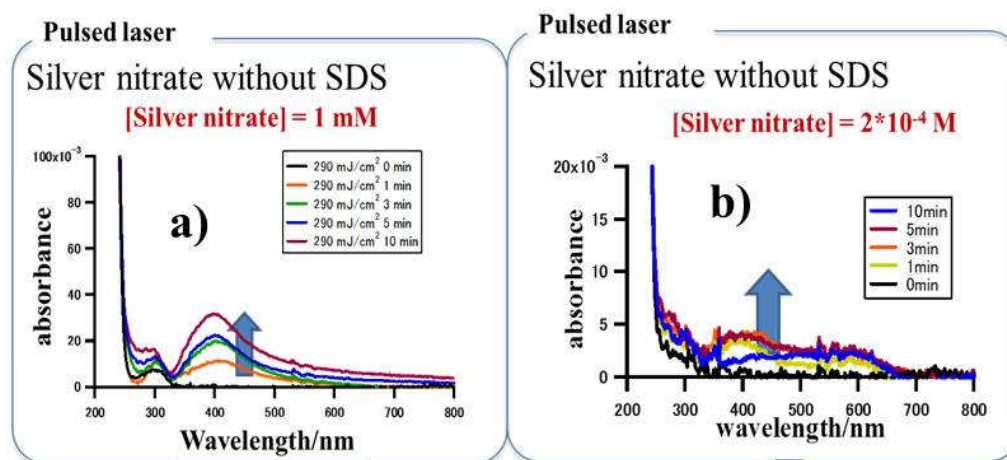


Figure 3.7 Absorption spectra showing nanoparticle growth: (a) [silver nitrate] = $1 \times 10^{-3} \text{ M}$; (b) [silver nitrate] = $2 \times 10^{-4} \text{ M}$. Laser intensity was 290 mJ/cm^2 for (a) and 300 mJ/cm^2 for (b).

At high concentration solution (without SDS: silver nitrate: 1 mM) we could not find the clear indication of absorption peak for NC's because a variety of photo-products

were formed along with NCs. According to the literature, NCs with 100 nm edge length have an absorption peak at 500 nm; however, the products had a broad absorption from 400 to 600 nm. Figure 3.7 (a) shows absorption peak at 405 that corresponds with small size spherical NPs while the long tail indicates the presence of AgNCs. An increase in absorption around 530 nm also indicates the increase in size of AgNCs. The absorption peak for AgNCs is not clear in case of higher concentration of silver nitrate due to increase in number of products in the solution. Figure 3.7 (b) shows the absorption peak at 405 that shifts towards the longer wavelength (530 nm) after 10 min irradiation. The formation of absorption peak at 530 nm corresponds with AgNCs and increase in size. We also drop-cast the sample solution on ITO glass for SEM analysis. It should be noted that the photoproducts at both concentrations were same. The absorbance peak height is small at low concentration means that the number of photoproducts is also very small and very difficult to observe the effect of laser intensity and irradiation time on it. Hence, 1 mM concentration is used to observe these effects on the photoproduct.

3.4 Effect of CW-UV light on the growth process of AgNCs

The aim of this experiment is to discuss possible mechanism of the formation and growth process of AgNCs. As shown in Section 3.3.6 NP could not be synthesized by

CW light irradiation. This result implies that the initial process of NP formation, namely the neutralization of silver ions, may include multi photonic process. In this section, NPs formed after pulsed laser irradiation which was irradiated with CW and changes after CW irradiation was observed with absorption spectroscopy. These results will also help us to reveal the mechanistic approach that how AgNCs enlarge their sizes? Is single photon absorbed by NPs and increase their size?

Initially, the sample solution (silver nitrate, 1 mM) was irradiated with 355 nm laser light for 15 sec and then continues irradiating with CW-UV light (348 nm \pm 10 nm, 2.5 mW/cm²).

3.4.1 Optical properties of NCs by CW light irradiation

When 1 mM silver nitrate aqueous solution was irradiated with 355 nm pulsed laser light for 15 sec, absorption peak was observed at 405 nm (abs = 0.005). After 15 sec irradiation of pulsed laser light, CW-UV light (348 nm) was introduced to irradiate the same sample solution. A clear peak shift towards the longer wavelength from 405 to 550 nm (red shift) was observed after 15 min CW light irradiation as shown in Figure 3.8 which indicates the morphological changes takes place inside the sample solution. The peak position continued to shift towards longer wavelength by 1 hour, and then the peak position is nearly constant at 550 nm even with further

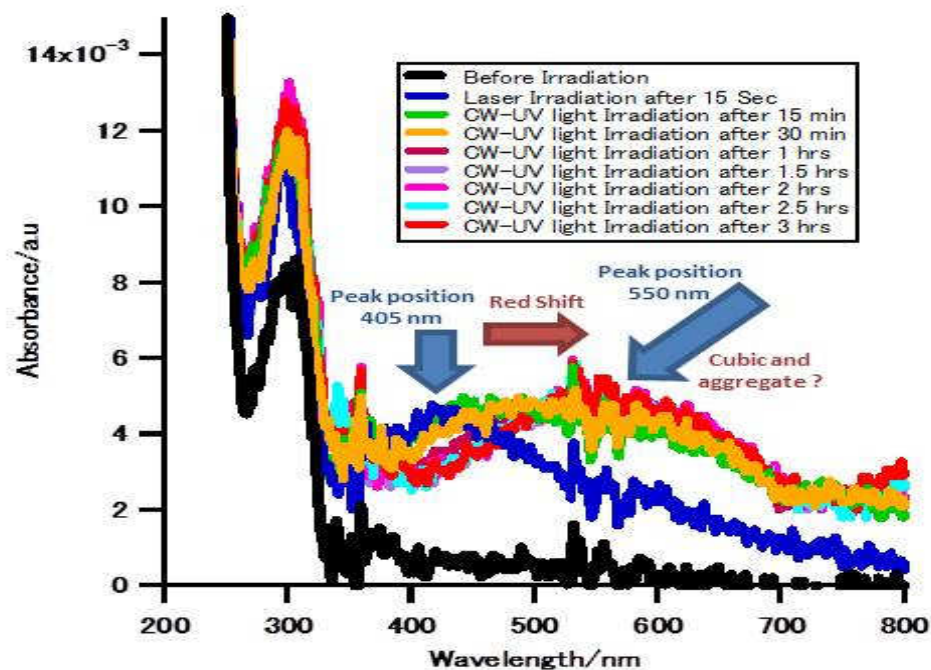
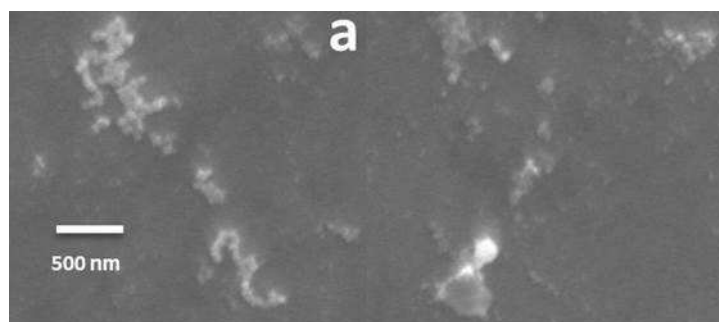


Figure 3.8 Evolution of the absorption spectrum of the silver nitrate solution irradiated first with pulsed laser for 15 sec and then irradiation with CW-UV light (348 nm) at various times

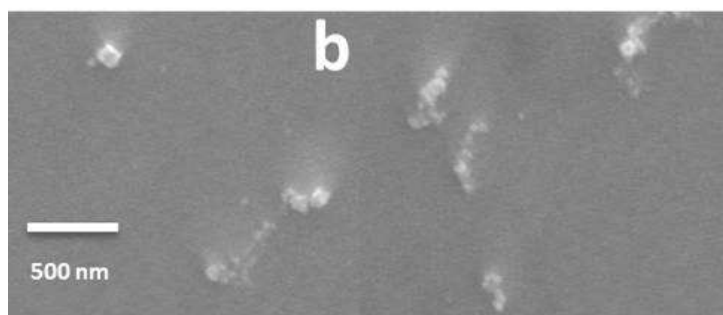
irradiation. Literature survey shows that this red shift may be due to the formation of different shapes and sizes or aggregation of nanoparticles [11]. To check what really happened by CW light irradiation, SEM images of product were taken.

3.4.2 SEM analysis of NCs after CW light irradiation

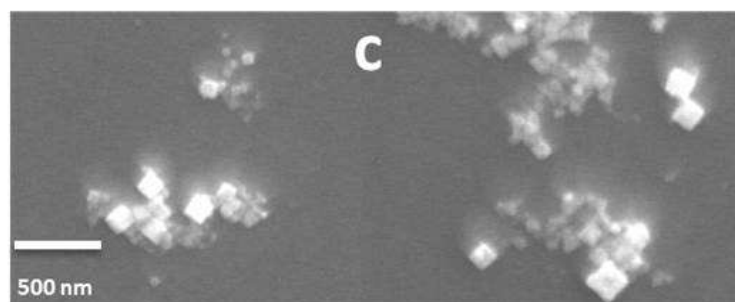
SEM photographs provided further insight into the morphology and size details of the silver nanoparticles. SEM images were taken after different irradiation time and corresponding with absorption spectra as shown in Figure 3.9 (a-d) and explain the growth process of silver nanoparticles. Initially, silver nanoparticles had round shape however, small aggregates were also formed (a). After 90 min CW-UV light irradiation, round shape NPs disappeared and turned into the cubic shape AgNPs. Which were bigger in size (Avg. 175 nm). Large asymmetric silver nanoparticles were formed after 3 hours along with the presence of cubic shape. It was also noticed that the size of AgNCs were also increased with time. These results are similar as we observed in the case of laser irradiation effect on the formation of AgNCs and give support to the explanation that single photon is absorbed by a particle and size increases[11]



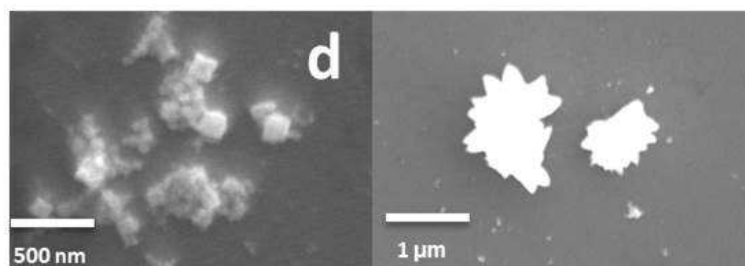
After 15 min CW-UV light (348) irradiation



After 60 min CW-UV light (348) irradiation



After 90 min CW-UV light (348) irradiation



After 120 min CW-UV light (348) irradiation

Figure 3.9 (a-d) SEM images taken after various irradiation time (CW-UV)

3.5 Conclusion

In this study, AgNPs were fabricated, using direct laser irradiation method, which differs from other laser processes such as the formation of AgNPs by pulsed laser ablation of a solid silver target immersed in a liquid. Photoreduction of silver ions present in the solution, leading to the formation of AgNPs, was initiated by nonlinear process. Log-log plot of absorbance vs laser intensity gave the slope value 1.5 which also confirmed the initial process was nonlinear. As a result, a variety of NPs were fabricated without using surfactants. We noticed that the number as well as size of AgNCs increased with laser intensity. The size distribution of AgNCs was investigated with various irradiation time and laser intensity. It revealed that NCs grow in their size with irradiation time and the growth process of AgNCs was highly depended on laser intensity. CW-UV light was also used to explain the growth process of AgNCs. On the basis of these results, we confirmed, AgNCs increased their size via single photon absorption.

3.5 References

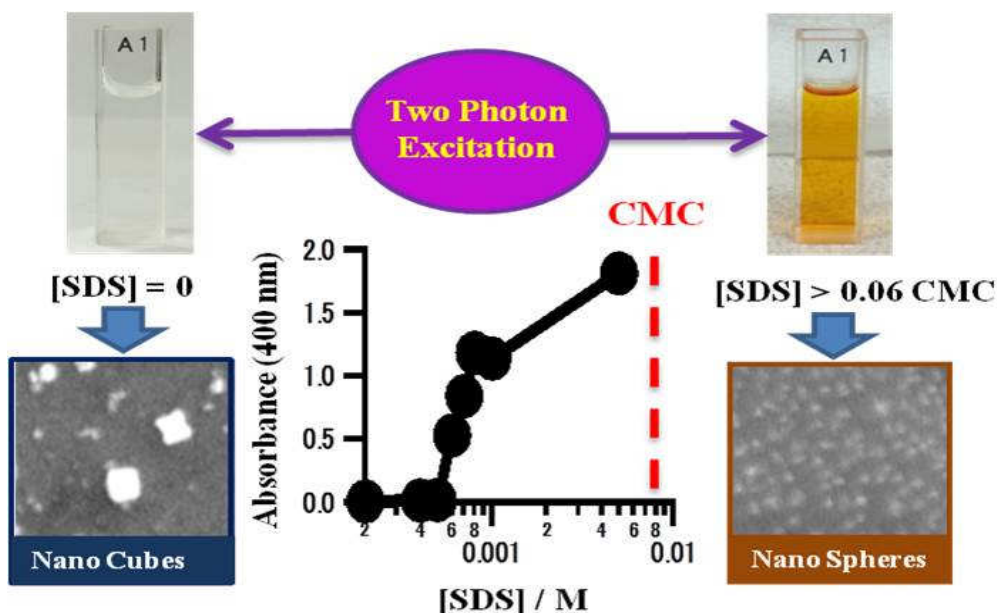
- [1] C. F. Bohren and D. R. Huffman, *Absorption and Scattering of Light by Small Particles*, Wiley, New York, 1983; Mir, Moscow, 1986.
- [2] N. G. Khlebtsov, L. A. Trachuk¹, A. G. Mel'nikov, *Optics and Spectroscopy*, **2005**, *98(1)*, 77.
- [3] Y. Yu, S. S. Chang, C. L. Lee, C. R. C. Wang, *J. Phys. Chem. B* **1997**, *101*, 6661.
- [4] Y. Sun, Y. Xia, *Science* **2002**, *298*, 2176.
- [5] K. G. Stamplecoskie, J. C. Scaiano, *J. Am. Chem. Soc.* **2010**, *132*, 1825.
- [6] T. Nakamura, H. Magara, Y. Herbani, S. Sato. *Appl. Phys. A* **2011**, *104*, 1021.
- [7] P. V. Kamat, M. Flumiani, G. V. Hartland, *J. Phys. Chem. B* **1998**, *102*, 3123.
- [8] A. Heilmann, A. Kiesow, M. Gruner, U. Kreibig, *Thin Solid Films*, **1999**, *175*, 343.
- [9] R. He, X. Qian, J. Yin, Z. Zhu, *J. Mater. chem.* **2002**, *12*, 3783.
- [10] F. Hubenthal, *Eur. J. Phys.* **2009**, *30*, S49.
- [11] A. Callegari, D. Tonti, M. Chergui, *Nano Lett.* **2003**, *3(11)*, 1565.

Chapter 4

Effect of sodium dodecyl sulfate on
the formation of silver nanoparticles
by biphotonic reduction of silver
nitrate in water

4.1 Abstract

Silver nanocubes (NCs) were found after irradiation of ns UV pulses into aqueous solution of silver nitrate. The photoproduct was turned to nanospheres (NSs) when solution contained a certain amount of SDS and irradiated. The SDS concentration to alter the photoproduct from NCs to NSs was about ten times lower than the critical micellar concentration (CMC) of SDS, which implies that a single layer of SDS adsorbed on silver surfaces assisted the growth of NSs which was explained in terms of hemi-micelle formation on charged surfaces.



Graphical Abstract

4.2 Introduction

In Chapter 3, I described, variety of AgNPs were fabricated by irradiating ns UV pulsed laser to aqueous solution of silver nitrate without using surfactants. We noticed that among these NPs, AgNCs increased their size along with laser intensity and irradiation time and discussed in detail [1]

Metallic nanoparticles (MNPs) have been used as markers, sensors, catalysts, sterilizers, and have applications in biomedical and pharmaceutical industries [2-4]. Mass production of MNPs has been achieved using wet chemical reduction by reducing metallic ions to metal and stabilizing them by a capping agent [5-7]. Capping agent and reducing agent must be removed before using MNPs to deal with contamination. To this end photo-reduction method of metal ions to metal has been worked out [8-10]. Reducing agents may work as capping agents affecting the shape of NPs. Addition of many chemicals can make the process complicate to understand the individual role of each additive [11-12]. I used photon instead of reducing agents for the investigation of surfactant effect on AgNPs.

As shown in the previous chapter, by using non-focused high intensity laser irradiation, NPs were successfully obtained. This technique allows us to make NPs without reducing agents. In this chapter, SDS was added as a stabilizing agent, and the role of

SDS was studied. Since we do not use any reducing agents, we can clarify the individual role of each surfactant. Application of this technique produced uniform NPs with lesser additives. Using this method we have clarified mechanism of NP formation. Sodium dodecyl sulfate (SDS) with variable concentrations was employed. Investigation showed the following results: (I) initial process was two photon ionization of water, (II) nanocubes (NCs) were obtained without surfactants, on the other hand, stable uniform nanospheres (NSs) were formed adding ten times low concentration of SDS compared to the critical micellar concentration (CMC) of SDS. Even at such low concentration of SDS, there are many SDS molecules but there is no special attractive force between SDS and NPs, and there is a dynamic equilibrium between free SDS and adsorbed SDS on NPs and can be explain by means of its critical hemi-micellar concentration (CHMC) [13-16].

4.3 Results and Discussion

4.3.1 Comparison of photo-product by SEM and their size distribution

In chapter 3, photoproducts without using any additives were discussed in detail. Here, we will make a comparison of photoproducts with and without using surfactant. Figure 4.1 shows typical SEM images of photoproducts formed by laser irradiation (355 nm, 290mJ/cm², 10 Hz, 10 min) to silver nitrate aqueous solution without (a) and

with (b) SDS (5×10^{-3} M). The initial concentration of silver nitrate was 1×10^{-3} M for (a) and 2×10^{-4} M for (b). Insets are particle size distributions: from SEM images (a); by DLS (b). Note that the distribution (a) counts only NCs. A variety of products and their aggregates were formed without SDS, including NCs which size increased with irradiation time. The addition of SDS markedly changed the photoproducts to homogeneous NSs with an average diameter of 14 nm.

These results suggest that a variety of shapes including NCs can be formed if silver atoms generated by photo-reduction of silver ions crystallize without any additives in water, and SDS would be solely responsible for shaping NSs. There are reports showing that NSs can be fabricated without SDS but with chemical reducing agents like glucose [17-18]. This result shows that glucose, the reducing agents can also work as capping agents in some cases to form specific NP shapes. It should be noted that the shape of NCs never turned to round but NCs simply grew in size by repetitive irradiation within 45 min. This growth of neat NCs indicates that the effect of transient melting yielding round shapes by intense lasers [19] would be negligible small.

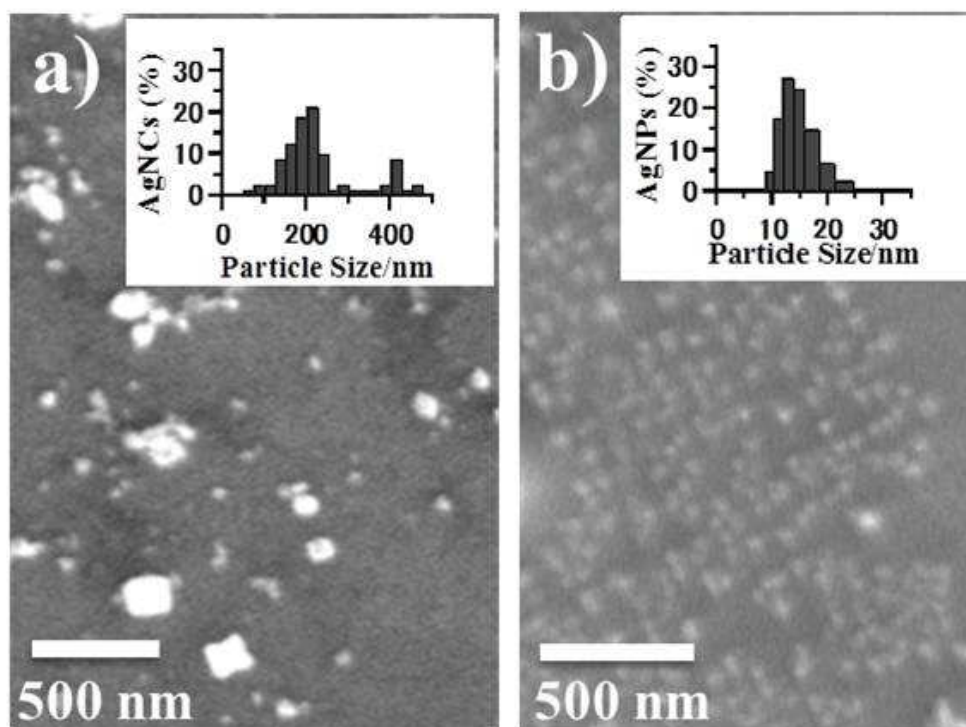


Figure 4.1 SEM images of nanoparticles formed by laser irradiation (355 nm, 290mJ/cm², 10 Hz, 10 min) to silver nitrate aqueous solution without (a) and with (b) SDS (5×10^{-3} M). The initial concentration of silver nitrate was 1×10^{-3} M for (a) and 2×10^{-4} M for (b). Insets are particle size distributions: from SEM images (a); by DLS (b). Note that the distribution (a) counts only NCs.

4.3.2 Optical properties

NP formation by repetitive laser irradiation was also confirmed with UV/vis. absorption spectra as shown in Figure 4.2 NSs having the absorption peak at about 400 nm didn't increase so much without SDS, while certain high concentrations of SDS assisted the NS increase. Interestingly, the absorption peak stopped its increase after a long term irradiation depending on the concentration of SDS and further irradiation just shifted the spectral shape to longer wavelengths. This means that NSs would start to aggregate, grow in size, or change shapes after a certain period of laser irradiation depending on a SDS concentration. When the concentration of SDS was high enough as shown in Figure 4.2 (c), a sharp increase at 400 nm without a peak shift was observed even at short irradiation time. The absorption spectra of nanoparticles shown in Figure 4.2 (c) did not change even after an irradiation time longer than 45 min (data were not shown, 60 min), which implies that the saturation of nanoparticle formation took place at this absorption value and all silver ions in solution were consumed.

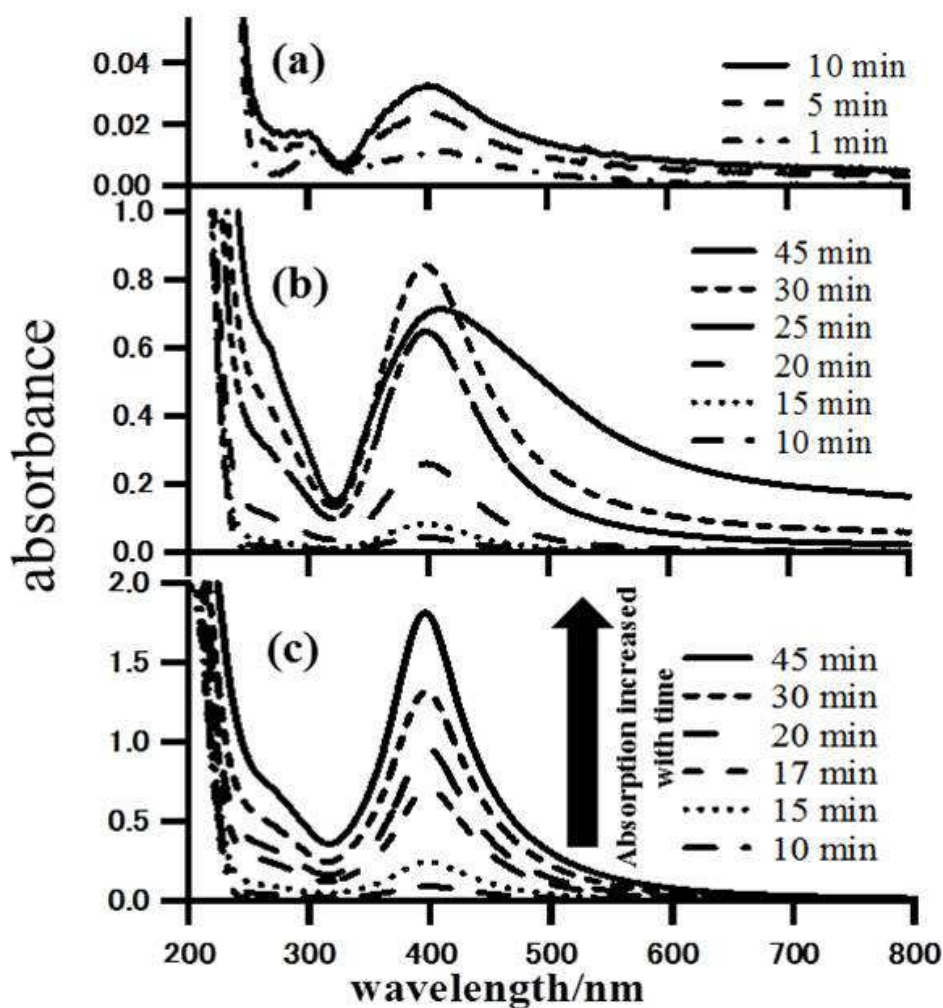


Figure 4.2 Absorption spectra showing increase in number of products: (a) without SDS; (b) $[SDS] = 7 \times 10^{-4} \text{ M}$; (c) $[SDS] = 5 \times 10^{-3} \text{ M}$. Laser intensity was 300 mJ/cm^2 for (a) and 290 mJ/cm^2 for (b) and (c). The initial concentration of silver nitrate was $1 \times 10^{-3} \text{ M}$ for (a) and $2 \times 10^{-4} \text{ M}$ for (b) and (c).

4.3.3 Estimation of molar absorption coefficient

Figure 4.3 clearly indicates that the maximum absorbance of nanoparticles after a long term irradiation was proportional to the original concentrations of AgNO_3 . Based on the above assumption, we were able to evaluate the molar absorption coefficient for a single atom in NSs to be $9000 \text{ M}^{-1}\text{cm}^{-1}$, which is in good agreement with the reported values ($4000 - 10000 \text{ M}^{-1}\text{cm}^{-1}$) reported for gold and silver alloy NPs [20].

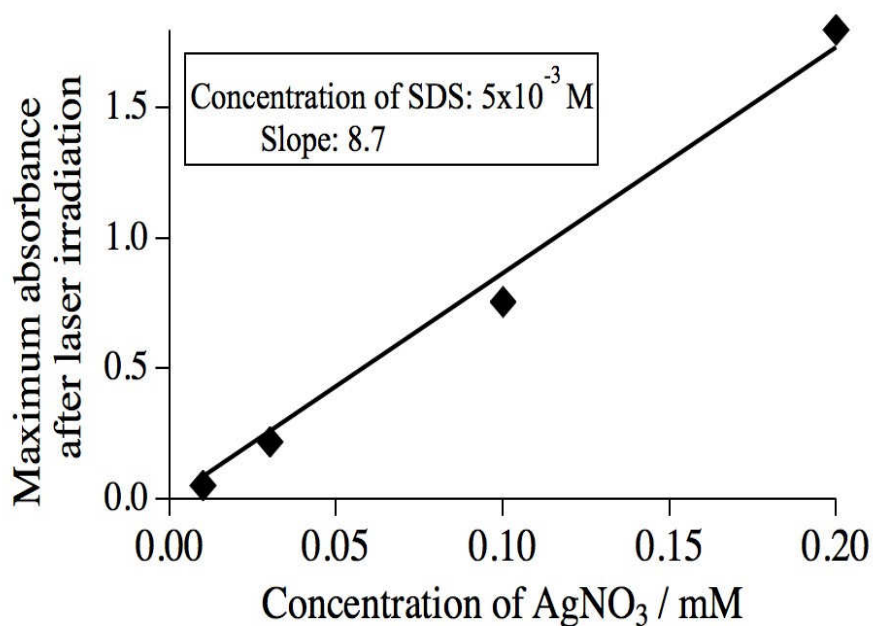


Figure 4.3 Maximum absorbance after laser irradiation ($300 \text{ mJ}/\text{cm}^2$) into a variety concentration of AgNO_3 aqueous solution containing $5 \times 10^{-3} \text{ M}$ SDS. The irradiation time for each concentration solution, which gave the maximum absorbance, was 45 min (for $1 \times 10^{-4} \text{ M}$, $2 \times 10^{-4} \text{ M}$), 60 min (for $3 \times 10^{-5} \text{ M}$) and 90 min (for $1 \times 10^{-5} \text{ M}$).

From the DLS data shown in Figure 4.4, we evaluated the average diameter of NSs to be 14 nm. By assuming the density of AgNP is the same as that of bulk silver, It was estimated that a single NS formed with 84000 atoms. I also assumed that all silver ions present in the solution converts into AgNPs. This allowed us to estimate an average molar absorption coefficient of NSs to be $7.6 \times 10^8 \text{ M}^{-1} \text{ cm}^{-1}$.

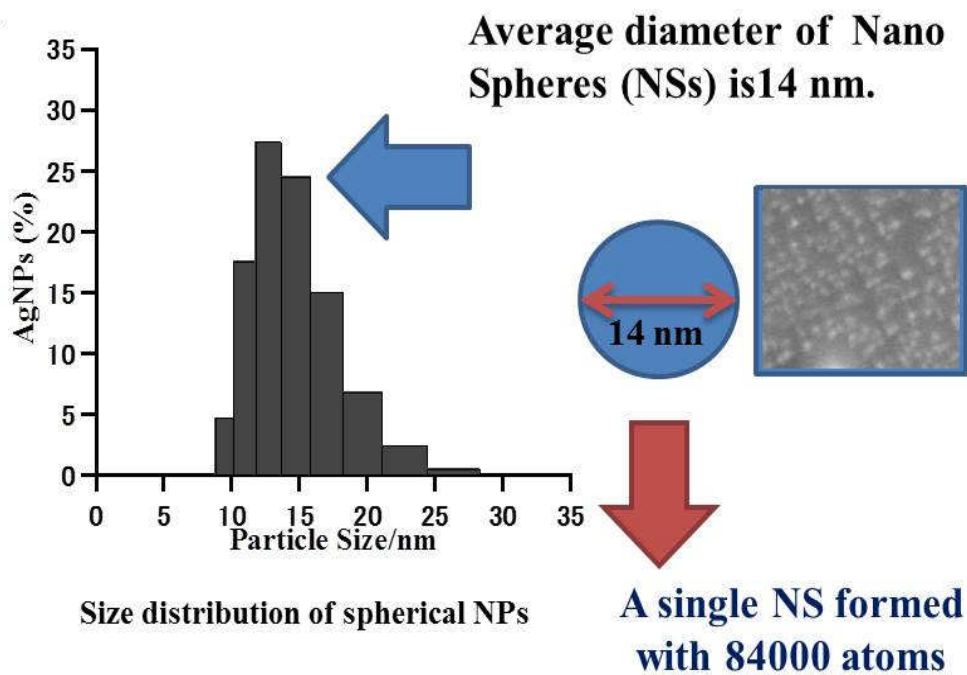


Figure 4.4 DLS results of size distribution of AgNSs. The average diameter of NS is 14 nm. A SEM photograph shows the formation of AgNS.

Table 4.1 shows the calculation values.

Size of nanoparticles: diameter:	14 nm (radius: 7nm)	7	nm
The volume of single nanoparticle:	$V=(4/3)\pi*r^3=1436.76 \text{ (nm}^3\text{)}$ $=1.4 \times 10^{-18} \text{ cm}^3$	1.43671E-18	cm ³
Number of Ag atoms in single NP:	$n = Vd/107.8682 \cdot R$	84142.94171	atoms/particle
	Density of bulk silver: $d = 10.49 \text{ g/cm}^3$		
	Avogadro's number: $6.022 \times 10^{23} \text{ atom/mole}$		
	Atomic mass of silver: 107.8682 g/mole		
Molar absorption coefficient of AgNP	$e = \text{Abs}/(c/n)$	757286475.4	M ⁻¹ ·cm ⁻¹
	Abs@1.0 x10 ⁻⁴ M AgNO ₃ : 0.9		

Table 4.1 Calculation for measuring the molar absorption coefficient

4.3.4 Stoichiometry of photoreaction

We also applied a high SDS condition to study the stoichiometry of this photoreaction. The absorption peak intensities after short time irradiation were plotted against laser intensities as shown in Figure 4.5. The slopes of the log-log plots satisfactorily give values around 2, which indicate that the initial stage of

NS production process is biphotonic

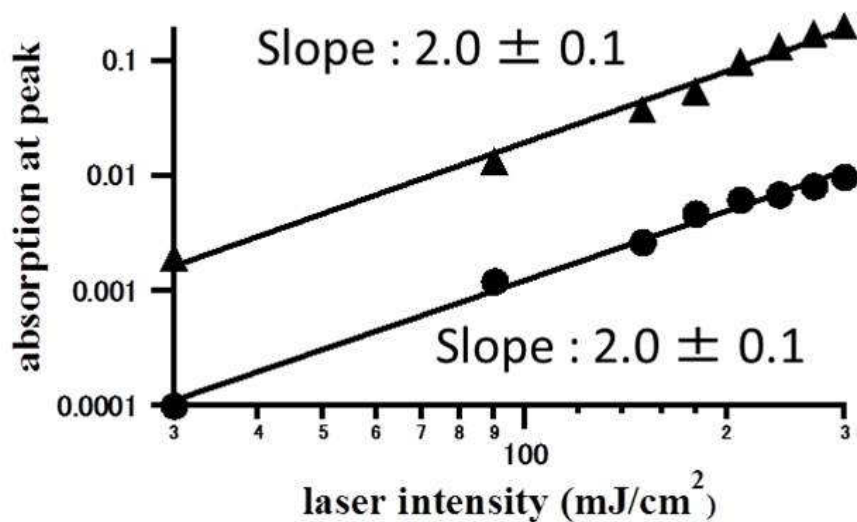
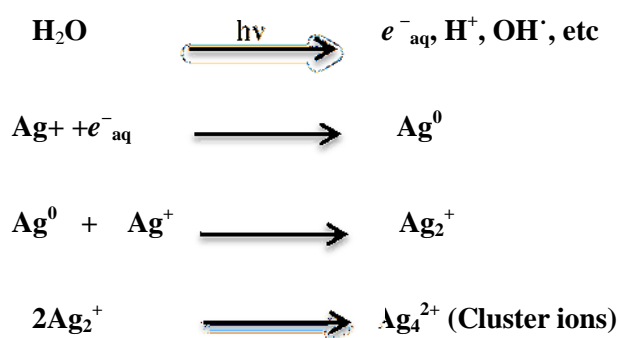


Figure 4.5 Absorbance at 400 nm after the irradiation of 15 s (circle) and 120 s (triangle) with different laser intensities. [Silver nitrate] = 10^{-3} M; [SDS] = 5×10^{-3} M.

This result suggests that the number of electrons ejected by two photon ionization of water determines the overall reaction yield of NS at short irradiation time. Such biphotonic ionization of water with intense UV pulses is well known process and its lowest ionization energy limit is obtained to be 6.5 eV, [21] which is slightly less than the double of the employed photon energy (3.49 eV) in this study. Once solvated electrons are produced, silver ions would be reduced and then form cluster ions like

Ag_4^{2+} , as known from pulse radiolysis studies [22-24]. These cluster ions can simply aggregate to form NPs with assistance of chemical reducing agents like radicals or additional photo-reduction.



NCs were also seemed to be form by a biphotonic process, although the stoichiometry of NCs can't be confirmed from absorption spectra. It is very likely that slow growth by the diffusion of low-concentration silver atoms could lead to the formation of neat cubic crystals. In our experiment, the laser beam was not focused into solution, thus causing no laser ablation nor plasma formation in solution. This homogeneous illumination allowed us to simplify occurring mechanism although the laser intensity was more than MWcm^{-2} . We believe that this experimental condition is more advantageous than those with focused laser beams which might complicate product

analysis [25-26]. In this sense, NP formation processes here may be similar to those in radiolysis rather than laser ablation to yield various fragments.

4.3.5 Time profile with various SDS concentrations on growth process

The effect of SDS was further examined with the observation of increases in NS number by measuring the absorption peak (400 nm) for a various concentration of SDS. The increase rate of NS became larger with SDS concentration and the maximum NS yield also increased likewise as shown in Figure 4.6. This implies that the growth of NS is supported by SDS molecules present in the solution and NSs would start to aggregate if the number of NSs exceeds a certain value limited by a SDS concentration.

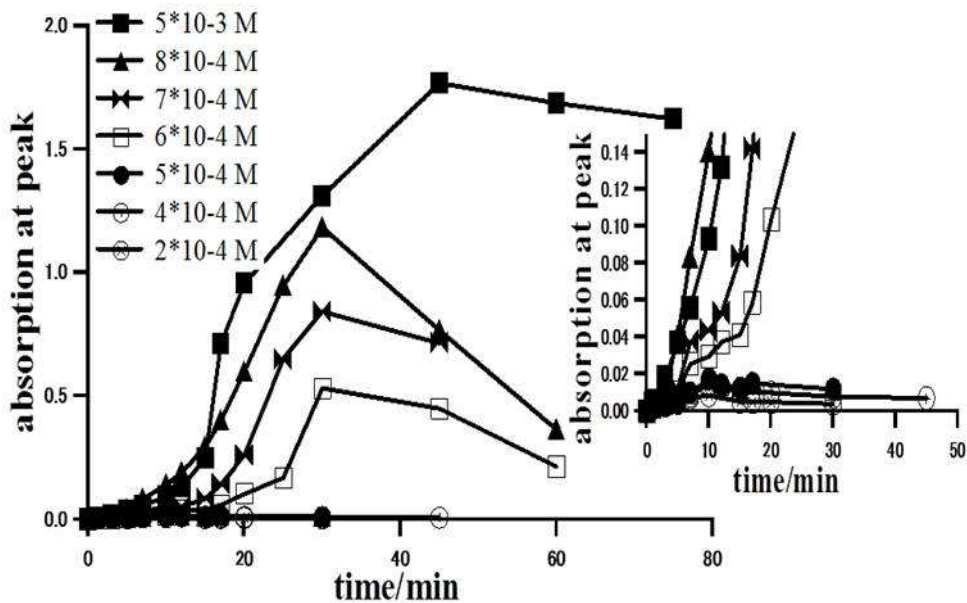


Figure 4.6 Growth of the peak absorbance with laser irradiation (300 mJ/cm^2). SDS concentrations varied from 2×10^{-4} - 5×10^{-3} M while keeping the concentration of silver nitrate at 2×10^{-4} M. The inset shows an enlarged image at a short time.

4.3.6 Effect of sodium methyl sulfate (SMS)

To exclude a possibility that NSs were simply formed by a specific interaction of silver atom or ions with sulfate ions, we performed similar experiments using sodium methyl sulfate and found no production of NS even with a high excess amount of the sulfate ions as shown in Figure 4.7. This result clearly indicates that the hydrophobic interaction between long alkyl chains of SDS molecules play an important role in the formation of NSs.

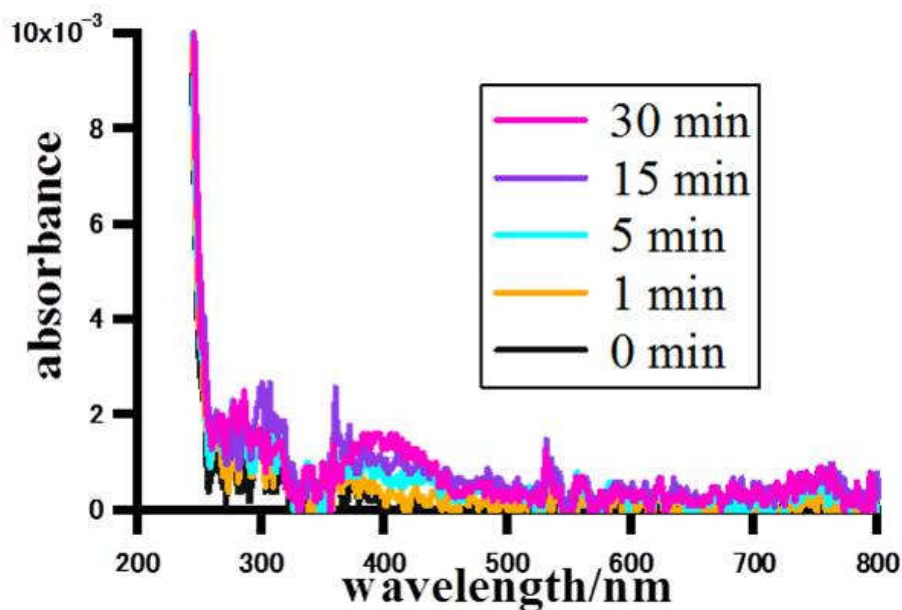


Figure 4.7 Absorption spectra of SMS (10^{-2} M) and silver nitrate (2×10^{-4} M) after different irradiation time

4.3.7 Effect of SDS concentration on NPs formation

Figure 4.8 shows a plot of the maximum yield of NSs as a function of SDS concentration. As the CMC of SDS is known to be 8.0×10^{-3} M, it is obvious that SDS supported the NS growth even with ten times below CMC. The lowest limit of the SDS concentration with which the NSs would start to grow fell in the range between 5×10^{-4} and 6×10^{-4} M. It is widely known that SDS can form small aggregates even below CMC, however, with the concentration of 5×10^{-4} M, 30% of SDS would form

antiparallel dimers and the others be only free monomers in aqueous solution [27-28].

It is thus not likely that SDS aggregates in solution works as a “template” of NSs.

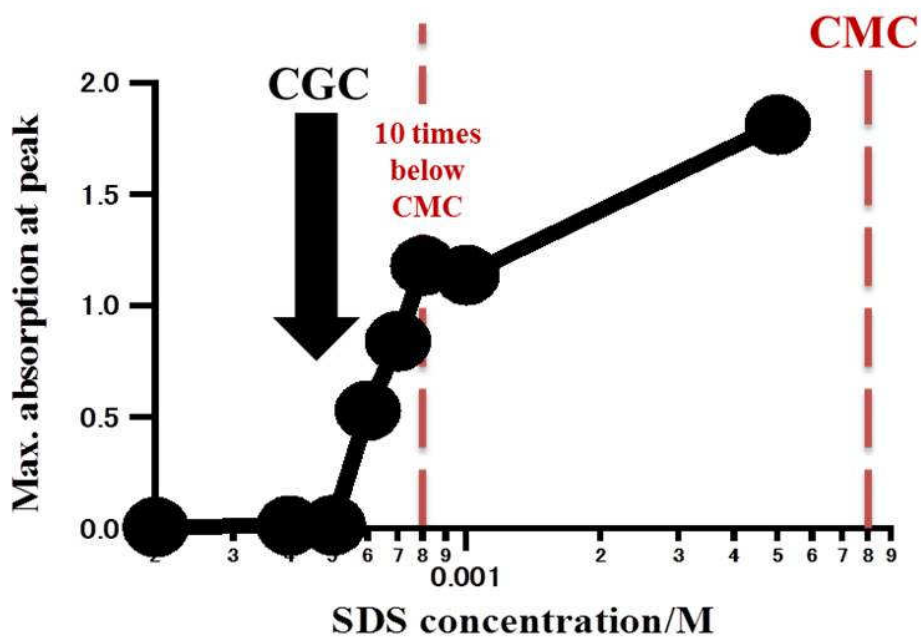


Figure 4.8 Maximum absorbance after ns laser irradiation (300 mJ/cm²) as a function of SDS concentration. The concentration of SDS varies from 2×10^{-4} to 5×10^{-3} M while silver nitrate concentration was kept constant (2×10^{-4} M). Arrow indicates the presence of critical growing concentration.

4.3.8 Role of SDS on growth process (Mechanism)

The role of SDS in supporting the growth of NSs with such a low concentration should be explained with the interaction between silver NS surfaces and SDS molecules as already pointed out [11]. It has been reported that SDS molecules form two-dimensional aggregates (hemi-micelles) at a water and charged alumina interface even with a low SDS concentration [12-14]. A variety of experimental techniques have revealed that SDS adsorption density on a positively charged surface abruptly increases around at a SDS equilibrium concentration that is about ten times lower than its CMC. The concentration, to form hemi-micelles at the interface, there are two regions depending on SDS concentration: 1) the region where the SDS adsorption density sharply increases due to the electrostatic attraction and additional lateral interactions between hydrocarbon chains; 2) the region where positively charged surfaces are neutralized by the adsorption of SDS and further gradual adsorption occurs with only hydrophobic interaction forming partly double layers at the interface. The transition between the two regions takes place around at a SDS equilibrium concentration about one order of magnitude lower than CMC, which is exactly corresponding to the critical growing concentration of NS in this experiment. Such SDS hemi-micellar formation on a positively charged electrode is also confirmed with

ellipsometry [13]. We thus presume that the growth of NS may be accelerated when positively charged silver surfaces are completely covered and neutralized by the adsorption of SDS monolayers.

4.3.9 Concept of hemi-micelle formation

For adsorption of ionic surfactants on oppositely charged surface, the adsorption isotherm called “Somasundaran–Fuerstenau” isotherm, plotted on a log–log scale, is typically characterized by four regions [29]. The main features of this type of adsorption isotherm are illustrated in Figure 4.9 for the adsorption of sodium dodecyl sulfate on alumina [30]:

Region 1. At low surfactant concentrations, the adsorption is due to electrostatic interaction between individual isolated charged monomeric species and the oppositely charged solid surface and the adsorption density follows the Gouy–Chapman equation with a slope of unity under constant ionic strength conditions.

Region 2. At the onset of region II, surfactant species begin to form surface aggregates, colloids (surface colloids), including hemi-micelles, admicelles, etc., due to lateral interactions between hydrocarbon chains. Due to this additional driving force resulting from the lateral association with the electrostatic interaction still active, the adsorption density exhibits a sharp increase in this stage

Region 3. When the solid surface is electrically neutralized by the adsorbed surfactant ions, the electrostatic attraction is no longer operative and adsorption takes place due to lateral attraction alone with a reduced slope.

Region 4. When the surfactant concentration reaches critical micelle concentration, the surfactant monomer activity becomes constant and any further increase in concentration contributes only to the micellization in solution and it does not change the adsorption density. The adsorption in this region is mainly through lateral hydrophobic interaction between the hydrocarbon chains. In regions 3 and 4, surfactant molecules adsorb with opposite orientation (head groups facing the bulk solution) resulting in a decrease in the hydrophobicity of the particles in this region.

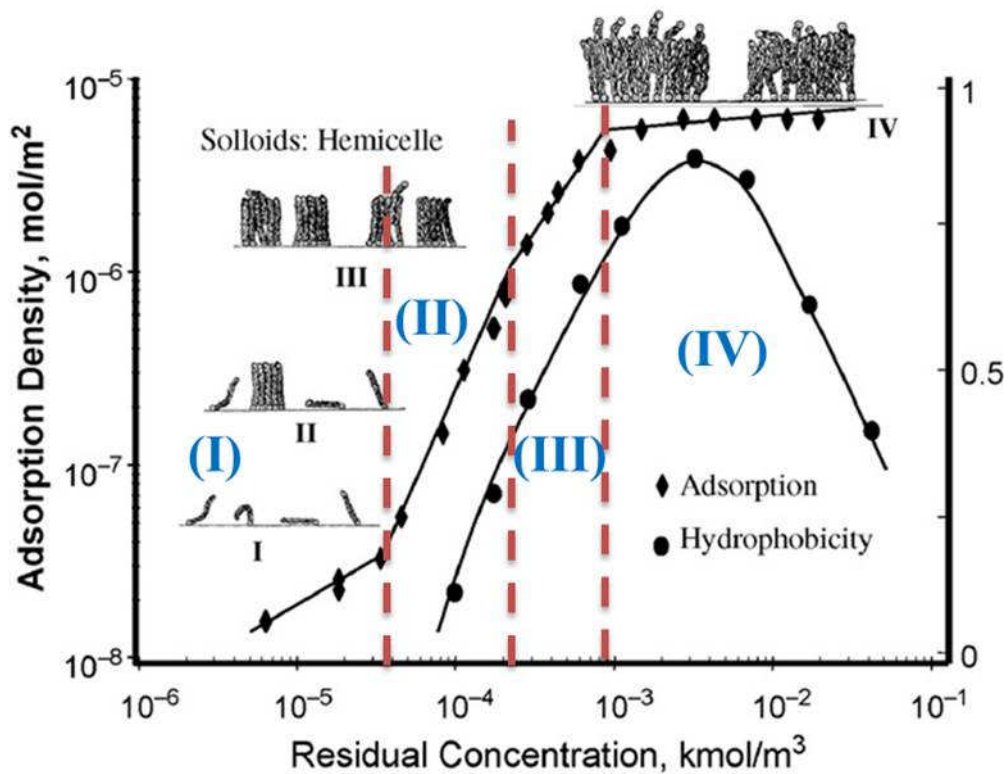


Figure 4.9 The adsorption isotherm, hydrophobicity of sodium dodecyl sulfate on alumina at pH 6.5. The attached illustrations show the growth of surface aggregates and orientation of surfactant molecules [29].

4.3.10 Number of SDS molecules required for single layer

The number of SDS molecules which are necessary to cover the whole NS surfaces with monolayers can be estimated from the average diameter and the number of NSs in solution. In our experimental condition, the complete photo-reduction of $2 \times$

10^{-7} M silver nitrate would yield NSs of 2.4×10^{-9} M. Each of NSs can be covered by roughly 3100 SDS molecules on the surface, which requires only 7.4×10^{-6} M of SDS. Consequently, the critical growing concentration we have observed in this experiment would be just a result of a dynamic equilibrium between adsorbed SDS and free abundant SDS in solution.

4.4 Summary and Conclusion

In conclusion, we have studied the effect of SDS on NP formation under a reducing-agent-free condition and then found that the photoproducts changed from NCs to NSs with a low concentration of SDS which is one order of magnitude lower than its CMC. The mechanism to change the shape of products is thought to be packed hemi-micellar formation of SDS molecules at silver NP surfaces, which neutralizes the surface charge of NPs.

4.5 References

- [1] U. Y. Qazi, D. Shirasawa, S. Kajimoto, H. Fukumura, 7th Asian Photochemistry Conference, **2012**, Osaka, Japan,
- [2] M. A. El-Sayed, *Acc. Chem. Res.* **2001**, *34*, 257.
- [3] S. Eustis, M. A. El-Sayed, *Chem. Soc. Rev.* **2006**, *35*, 209.
- [4] M. Rycenga, C. M. Cobley, J. Zeng, W. Li, C. H. Moran, Q. Zhang, D. Qin, Y. Xia, *Chem. Rev.* **2011**, *111*, 3669.
- [5] A. Tao, P. Sinsersuksakul, P. Yang, *Angew. Chem. Int. Ed.* **2006**, *45*, 4597.
- [6] J. Zeng, Y. Zheng, M. Rycenga, J. Tao, Z. Y. Li, Q. Zhang, Y. Zhu, Y. Xia, *J. Am. Chem. Soc.* **2010**, *132*, 8552.
- [7] A. Lo'pez-Miranda, A. Lo'pez-Valdivieso, G. Viramontes-Gamboa, *J. Nanopart. Res.* **2012**, *14*, 1101.
- [8] H. Hada, Y. Yonezawa, Y. Akio, A. Kurakake, *J. Phys. Chem.* **1976**, *80*, 2728.
- [9] K. Kurihara, J. Kizling, P. Stenius, J. H. Fendler, *J. Am. Chem. Soc.* **1983**, *105*, 2574.
- [10] S. Kajimoto, D. Shirasawa, N. N. Horimoto, H. Fukumura, *Langmuir* **2013**, *29*, 5889.
- [11] M. P. Pileni, *Nat. Mater.* **2003**, *2*, 145.

- [12] B. Wiley, Y. Sun, Y. Xia, *Acc. Chem. Res.* **2007**, *40*, 1067.
- [13] P. Somasundaran, D. W. Fuerstenau, *J. Phys. Chem.* **1966**, *90*, 70.
- [14] G. J. Besio, R. K. Prud'homme, J. B. Benziger, *Langmuir* **1988**, *4*, 140.
- [15] S. Paria, K. C. Khilar, *Adv. Colloid Interface Sci.* **2004**, *110*, 75.
- [16] R. Zhang, P. Somasundaran, *Adv. Colloid Interface Sci.* **2006**, *123–126*, 213.
- [17] S. Panigrahi, S. Kundu, S. K. Ghosh, S. Nath, T. Pal, *J. Nanopart. Res.* **2004**, *6*, 411.
- [18] J. Soukupová, L. Kvítek, A. Panáček, T. Nevěčná, R. Zbořil, *Mat. Chem. Phys.* **2008**, *11*, 77.
- [19] S. Link, C. Burda, B. Nikoobakht, M. A. El-Sayed, *J. Phys. Chem. B* **2000**, *104*, 6152.
- [20] S. Link, Z. L. Wang, M. A. El-Sayed, *J. Phys. Chem. B* **1999**, *103*, 3529.
- [21] D. N. Nikogosyan, A. A. Oraevsky, V. I. Rupasov, *Chem. Phys.* **1983**, *7*, 131.
- [22] A. Henglein, *Chem. Rev.* **1989**, *89*, 1861.
- [23] T. Linnert, P. Mulvaney, A. Henglein, H. Weller, *J. Am. Chem. Soc.* **1990**, *112*, 4657.
- [24] A. Henglein, M. Giersig, *J. Phys. Chem. B* **1999**, *103*, 9533.
- [25] J. P. Abid, A. W. Wark, P. F. Brevet, H. H. Girault, *Chem. Comm.* **2002**, 792.

- [26] T. Nakamura, H. Magara, Y. Herbani, S. Sato. *Appl. Phys. A* **2011**, *104*, 1021
- [27] Yu. F. Zuev, R. Kh. Kurbanov, B. Z. Idiyatullin, O. G. Us'yarov, *Colloid J.* **2007**, *69*, 444.
- [28] B. Z. Idiyatullin, K. S. Potarikina, Yu. F. Zuev, O. S. Zueva, O. G. Us'yarov, *Colloid J.* **2013**, *75*, 532.
- [29] L. K. Koopal, E. M. Lee, M. R. Böhmer, *J. Colloid Interface Sci.* **1995**, *170*, 85.
- [30] P. Somasundaran, D. W. Fuerstenau, *J. Phys. Chem.* **1966**, *70*, 90.

Chapter 5

Effect of additives on photo-products

5.1 Introduction

AgNPs were synthesized following the preparation procedure described in experimental section chapter 2. As a silver salt precursor, silver nitrate was dissolved in ultra-pure water and made a required sample solution (2×10^{-4} M). Researchers adopted various methods to synthesize NPs using surfactants [1-11]. AOT and some other additives SOS, SHS, SMS and BPPD were introduced in this experiment in place of SDS as discussed in the previous chapter. I will discuss the products of each additive one by one. AOT has CMC as 1.4×10^{-3} M [12]. I kept the silver salt concentration constant in all experiments however, AOT concentration varies from 3.5×10^{-5} - 7×10^{-4} M. Molecular structure of AOT has 20 carbon atoms which make long hydrocarbon chains and sulfate group attached at the center. Different molecular structure may have different effect on growth and size of synthesized product. Keeping these points in my mind, detailed experiments were performed and results are shown in detailed here. Comparison between SDS and AOT is also discussed.

5.2 Results and discussion

5.2.1 Optical properties [Aerosol OT (AOT)]

Sample solution was transparent before laser irradiation however; it turned into pale yellow indicating that AgNPs were formed. Figure 5.1 shows the photographs of

samples obtained before and after laser irradiation. Figure 5.2 shows absorption spectra after various irradiation times. A surface plasmon absorption band with a maximum peak at 396 nm indicates the presence of spherical AgNPs. It is confirmed by previous researchers that the absorption peak at 395 nm correspond with small sized spherical nanoparticles having the particle size in the range of 1-10 nm [13-18]. It was noticed into the absorption spectra that the absorption peak at 396 nm did not increase without AOT concentration, while increased with AOT increase.

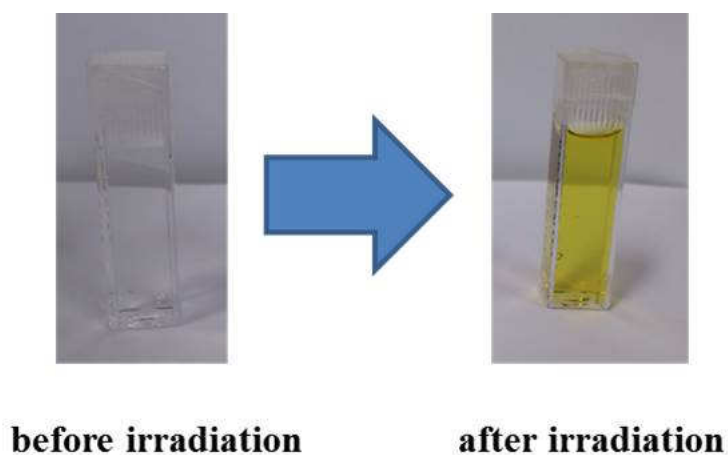


Figure 5.1 Photographs taken before and after ns laser irradiation. Transparent color of sample solution turned into pale yellow. The sample was 0.2 mM AgNO₃ aqueous solution with 0.7 mM AOT.

Absorption spectra did not show any shift means that synthesized products did not grow in size during laser irradiation. The absorption peak stopped its increase after a long term irradiation depending on the concentration of AOT and then further irradiation just shifted the spectral shape to longer wavelengths indicating red line after 60 min irradiation as shown in Figure 5.2 (a). This means that NSs would start to aggregate, grow in size, or change shapes after a certain period of laser irradiation depending on AOT concentration ($<.7 \times 10^{-4}$ M). The absorption spectra of nanoparticles shown in Figure 5.2 (b) did not change even 60 min irradiation time, which means that the saturation of nanoparticle formation took place at this absorption value and all silver ions in solution were consumed.

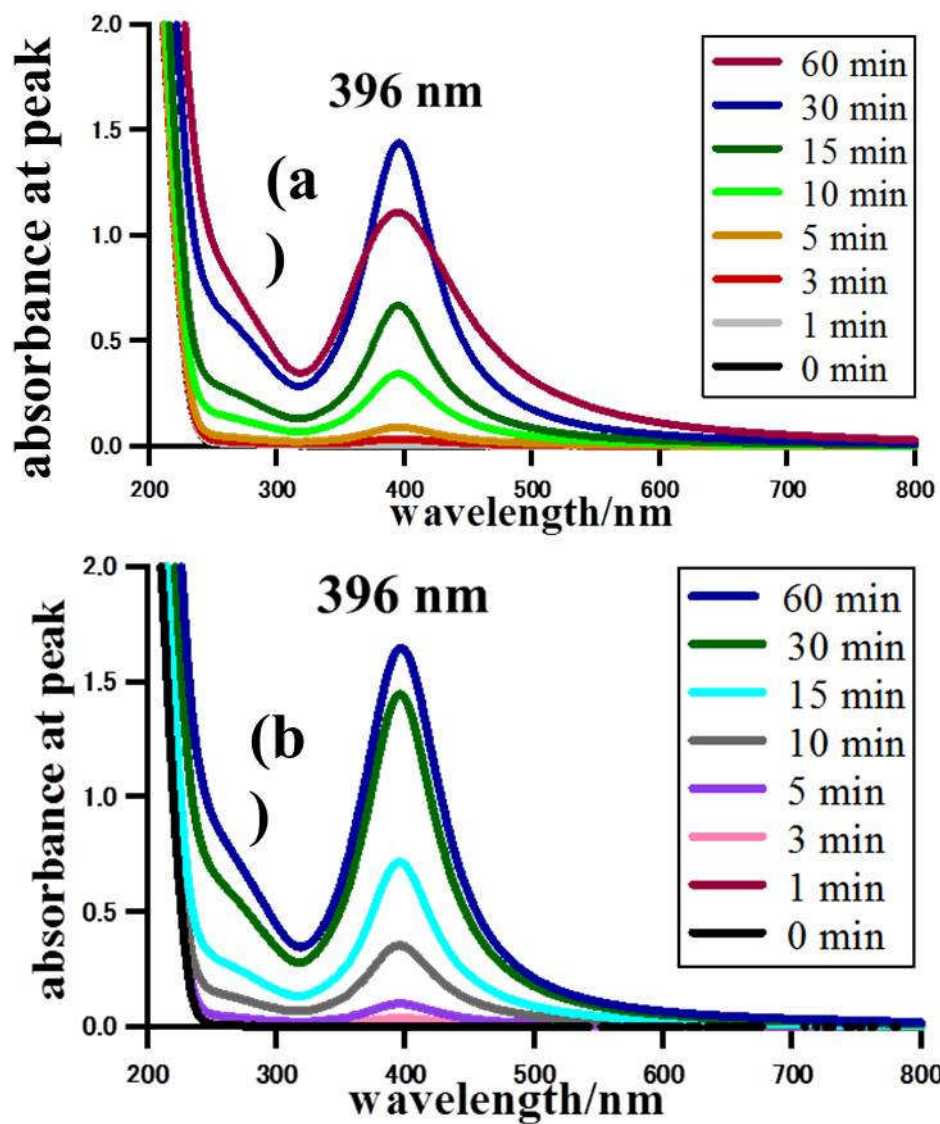


Figure 5.2 Absorbance spectra showing nanoparticle growth: (a) $[AOT] = 2 \times 10^{-4}$ M;

(b) $[AOT] = 7 \times 10^{-4}$ M. Laser intensity was 300 mJ/cm^2 and the silver nitrate

concentration was 2×10^{-4} M.

5.2.2 Time profile of AOT with various concentrations

Figure 5.3 shows the time profile of AgNPs growth assisted by various AOT concentrations; (a) indicates the growth process on short time window and (b) shows the growth of AgNPs on long time window. The results from absorption spectra clearly indicate that NPs increased with high AOT value in the solution however; there is a certain value which does not support the growth process. Above this concentration, the absorbance dramatically increased which is in line with SDS results. This implies that the growth process is supported by AOT molecules adsorbed on the surface of NPs. It was also noticed that the AOT value below 10 times lower than the CMC could not support the growth process which exactly same trend as observed in the case of SDS and discussed in detailed. I believe that the growth process should be discussed in the same manner as SDS.

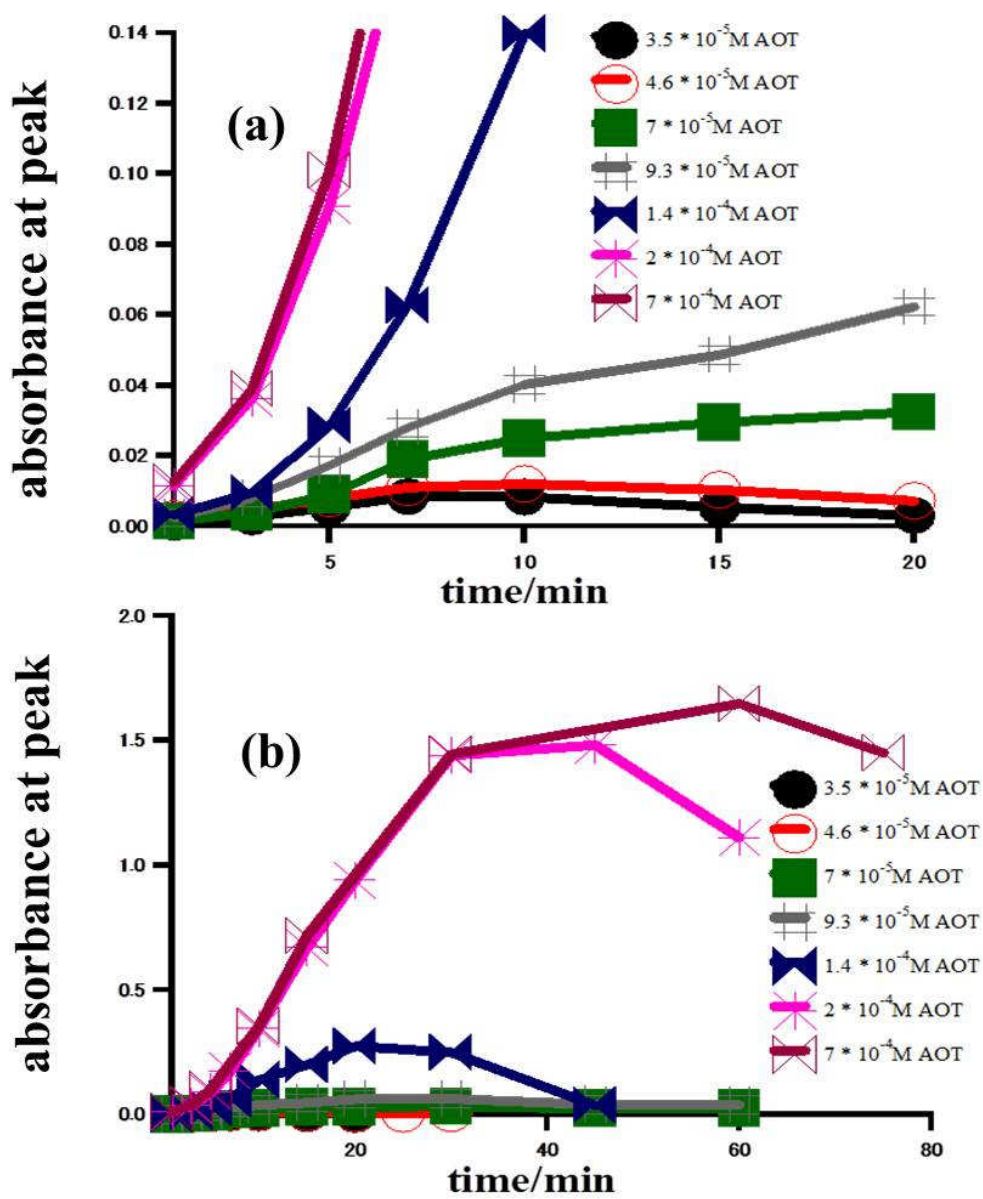


Figure 5.3 Growth of the peak absorbance with UV laser irradiation (300 mJ/cm²).

AOT concentration varies from 3.5×10^{-5} – 7×10^{-4} M while silver nitrate concentration is 2×10^{-4} M. (a) shows the enlarged image at short time scale (b) shows the results with long time scale.

5.2.3 Effect of AOT concentration on NPs formation process

Figure 5.4 shows a plot of maximum absorption peak as a function of various AOT concentrations. The arrow indicates the lowest limit of AOT concentration at which the growth of NP increased. This value is 10 times lower than the CMC (1.4×10^{-3} M) as comparable with the results of SDS. The lowest limit of the concentration at which the growth process would start to grow fell in the range 9.3×10^{-5} and 1.4×10^{-4} M. It is widely known that below CMC mostly surfactant molecules would form dimers and free monomers in aqueous solution [19-20]. At CMC, formation of soft templates in the solution takes place [21-24] while the surfactants with a concentration lower than CMC does not behave like a soft template. These results support the concept of hemi-miceller formation into the solution as discussed in detailed in chapter 4.

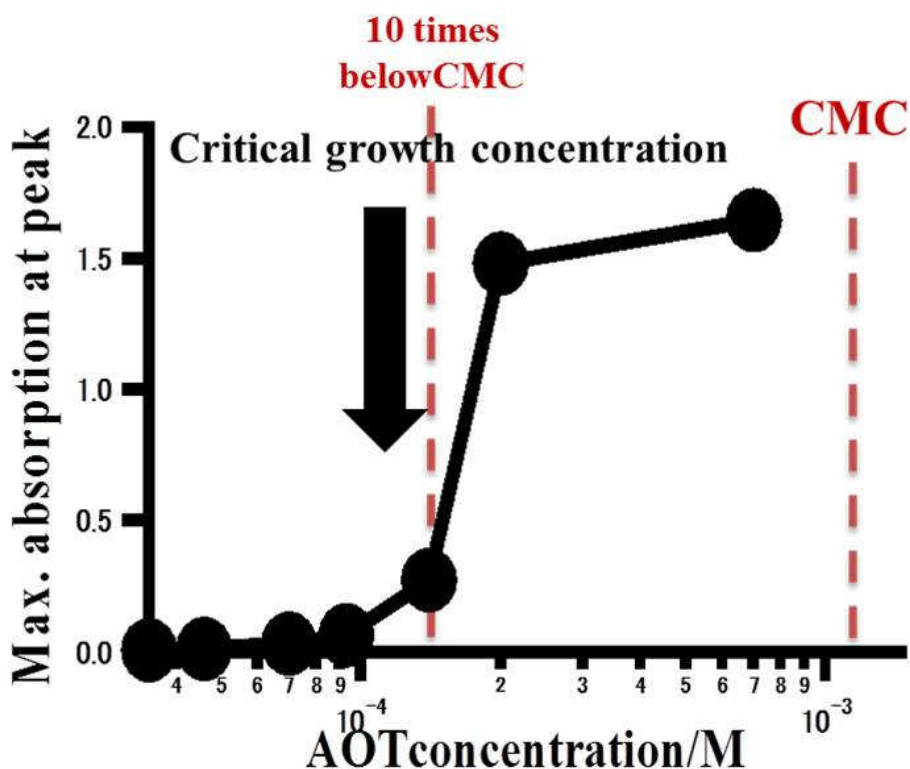


Figure 5.4 Maximum absorbance as a function of AOT concentration. The AOT concentration varies from 3.5×10^{-5} – 7×10^{-4} M while silver nitrate concentration kept same as 2×10^{-4} M. Arrow indicates the presence of critical growing concentration.

5.2.4 Comparison between SDS and AOT

On the bases of SDS and AOT, results clearly indicate the presence of certain value above which the NPs start to grow. It should be explained with the interaction between silver NS surfaces and surfactant molecules as already pointed out that SDS

molecules form two-dimensional aggregates (hemi-micelles) at a water and alumina interface even with a low SDS concentration [25-27]. AOT has two hydrocarbon chains, while SDS has single chain and the stability of the products is very different in both cases. With AOT, it is not stable. Based on absorption spectra, the size of products are also different as AOT gives smaller NPs. It is because of bulky alkyl chain of AOT. AOT has double alkyl chain and needs larger area when it absorbed on a AgNP even the size of head group is the same. That means, the cone angle of AOT is larger than SDS. This difference may change the size of products. The results are comparable with each other and support the concept of hemi-micelle formation as discussed by P. Somasundaran, [28]. According to the best of our knowledge, this is the first time to discuss the effect of surfactants on the growth process of NPs even at ten times lower than the critical micelle concentration (CMC) [29].

5.3 Sodium octyl sulfate (SOS)

5.3.1 Optical properties and SEM analysis

When aqueous solution of silver nitrate containing SOS at various concentrations were irradiated with ns laser light at different times, a surface plasmon absorption band with a broad range 400-600 nm was observed. It increased with time, reached saturation and then decreased. The absorption spectra of AgNPs obtained after various

irradiation times are given in Figure 5.5. Broad absorption spectra indicate the presence of wide range of shape and size distribution of AgNPs. The absorption spectra also indicate the formation yield increased with an increase in SOS concentration. The shape of the product is confirmed by SEM images as shown in Figure 5.6. The SEM images show that the photo-product had a wide range of shape and size distribution. Most of the particles has irregular in shape along with spherical and square shape. The irradiated sample solution was not stable and settled down due to aggregation of NPs.

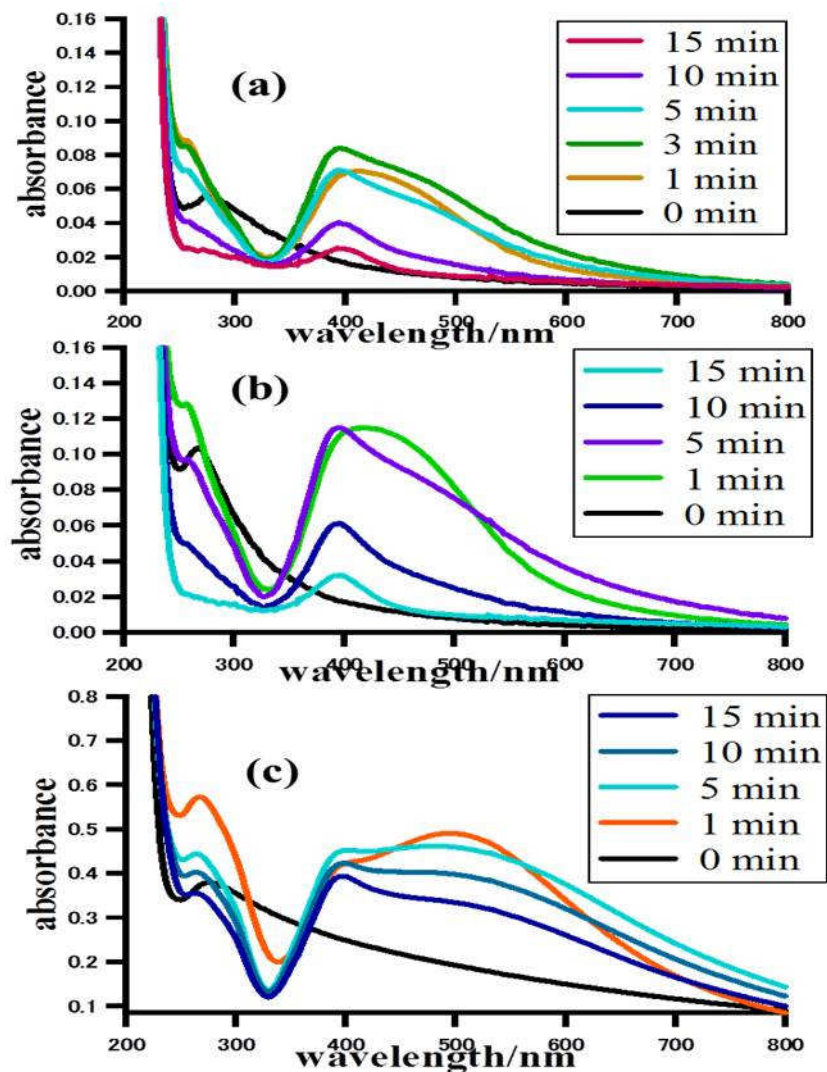


Figure 5.5 Absorbance spectra of SOS after laser irradiation (300 mJ/cm^2). (a) $[\text{SOS}] = 14 \times 10^{-3} \text{ M}$; (b) $[\text{SOS}] = 7 \times 10^{-3} \text{ M}$; (c) $[\text{SOS}] = 140 \times 10^{-3} \text{ M}$. silver nitrate concentration kept constant ($2 \times 10^{-4} \text{ M}$).

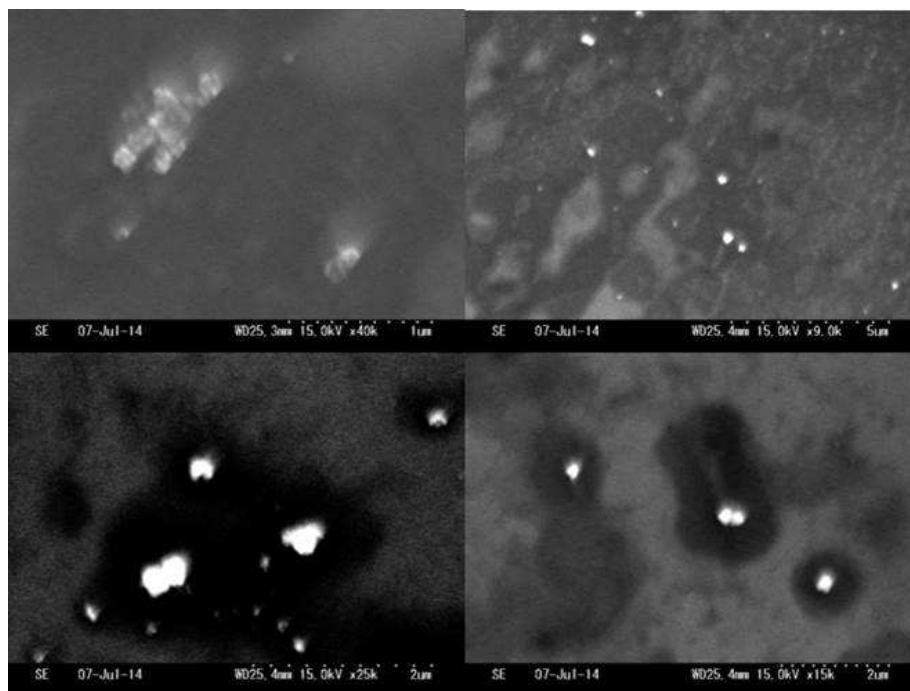


Figure 5.6 SEM images taken after different irradiation times while [SOS] = 3 mM in this caption.

5.3.2 SOS concentration effect on NPs

Figure 5.8 shows a plot of the maximum yield of NPs as a function of SOS concentration while the CMC value of SOS is 139 M [12]. The absorption spectra do not show the CGC value as observed in the case of AOT and SDS. On the basis of this result, it was concluded that the hydrocarbon chain plays an important role in the formation process. For further confirmation, the effect of hydrocarbon chain on the

formation process different molecules having short carbon chain was introduced. In

coming sections, I will discuss the effect of carbon chain using SHS and SMS.

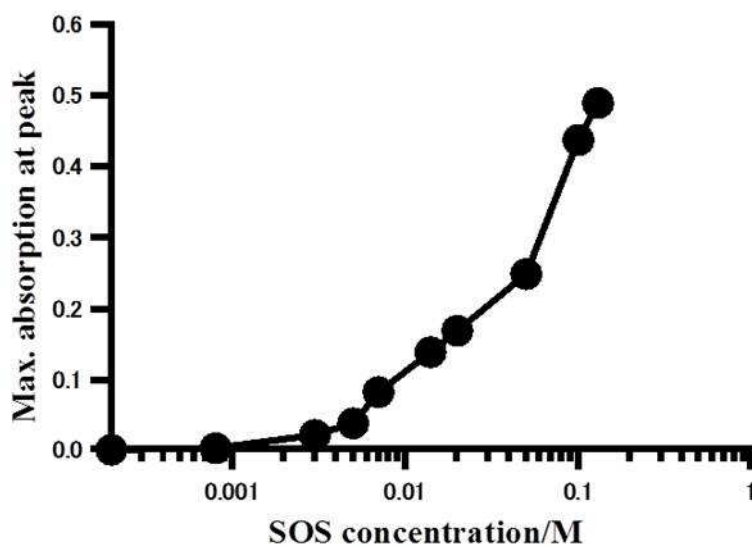


Figure 5.7 Maximum absorbance at various SOS concentrations. The concentration varies from 2×10^{-4} M to 0.13 mM while keeping silver nitrate concentration constant (2×10^{-4} M)

5.4 Sodium hexyl sulfate (SHS)

5.4.1 Optical properties and SEM analysis

When aqueous solution of silver nitrate containing SHS at various concentrations was irradiated with ns laser light at different times, a surface plasmon absorption band with a broad range from 350 to 700 nm was observed as shown in

Figure 5.8. The yield of products is very low even at very high concentration (0.42 mM) of SHS but compared to the results without additives, the yield is high. SHS molecule has short hydrocarbon chain. This result indicates that SHS molecules do not support the growth process of AgNPs. Below the CMC the absorption spectra is broaden however at CMC (.42 mM) a strong absorption peak is observed after 1 min irradiation at 425 nm which decreased afterward. It means that the AgNPs are not stable enough to keep for long time. The shape of the product was confirmed by SEM images as shown in Figure 5.9. The SEM images shows that spherical NPs were formed initially which have large size and precipitate out quickly. It also indicates that SHS does not have ability to support the formation process or increase the product yield even at very high concentration of SHS.

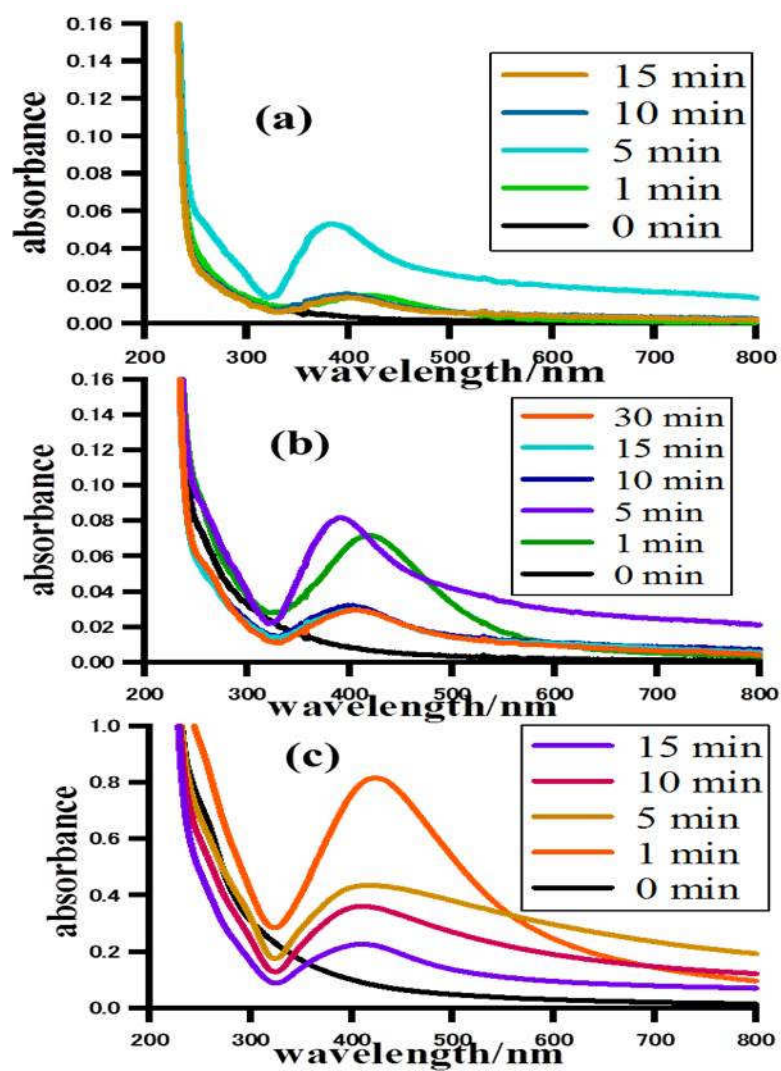


Figure 5.8 Absorbance spectra of SHS after laser irradiation (300 mJ/cm^2). (a) $[\text{SHS}] = 0.021 \text{ M}$; (b) $[\text{SHS}] = 0.042 \text{ M}$; (c) $[\text{SHS}] = 0.42 \text{ M}$. silver nitrate concentration kept constant ($2 \times 10^{-4} \text{ M}$).

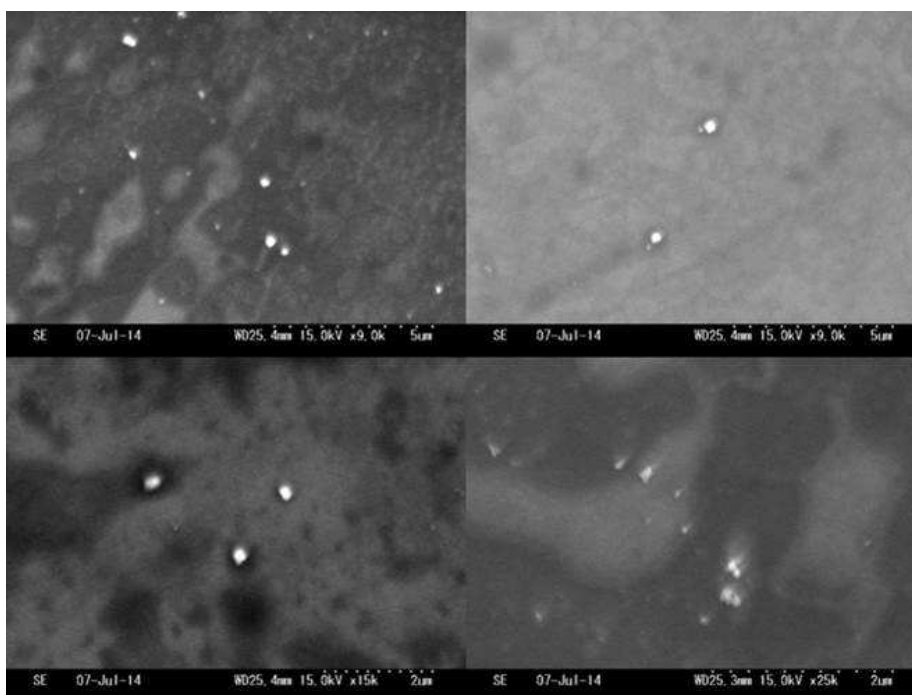


Figure 5.9 SEM image shows the formation AgNPs. SEM images are taken after 1 min irradiation times. While [SHS] = 0.042 mM.

5.5 Sodium methyl sulfate (SMS)

5.5.1 Optical properties and SEM analysis

Figure 5.10 shows the absorption spectra of SMS after laser irradiation. Silver nitrate was dissolved in an aqueous solution of silver nitrate (2×10^{-4} M). Sample solutions were prepared with various concentrations of SMS and irradiation with ns laser (300 mJ/cm^2). No prominent change in absorption spectra was observed even

after a high concentration (50 mM) of SMS. It means that SMS does not take part in the growth of AgNPs. The absorption looks similar to the absorption spectra of silver nitrate without using additives. Figure 5.11 shows the SEM images. Cubic shape NPs were observed along with irregular and round shape nano particles. Among these NPs the cubic shape of nanoparticles is little prominent. These results are same as in case of silver nitrate without using additives. Hence, we can say that SMS stay away in the formation process.

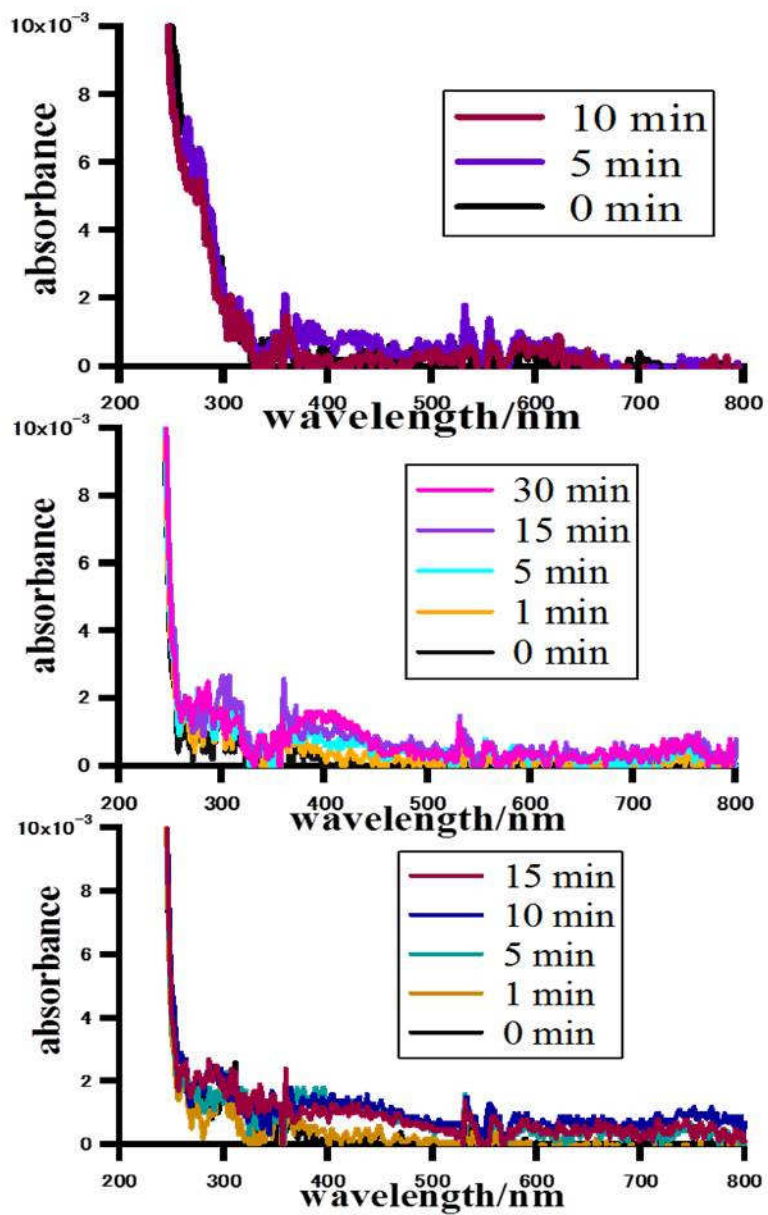


Figure 5.10 Absorbance spectra of SMS-AgNO₃ solution after laser irradiation (300 mJ/cm²). (a) [SMS] = 50×10⁻³ M; (b) [SMS] = 10×10⁻³ M; (c) [SMS] = 5×10⁻⁴ M. The concentration of silver nitrate was kept constant (2×10⁻⁴ M).

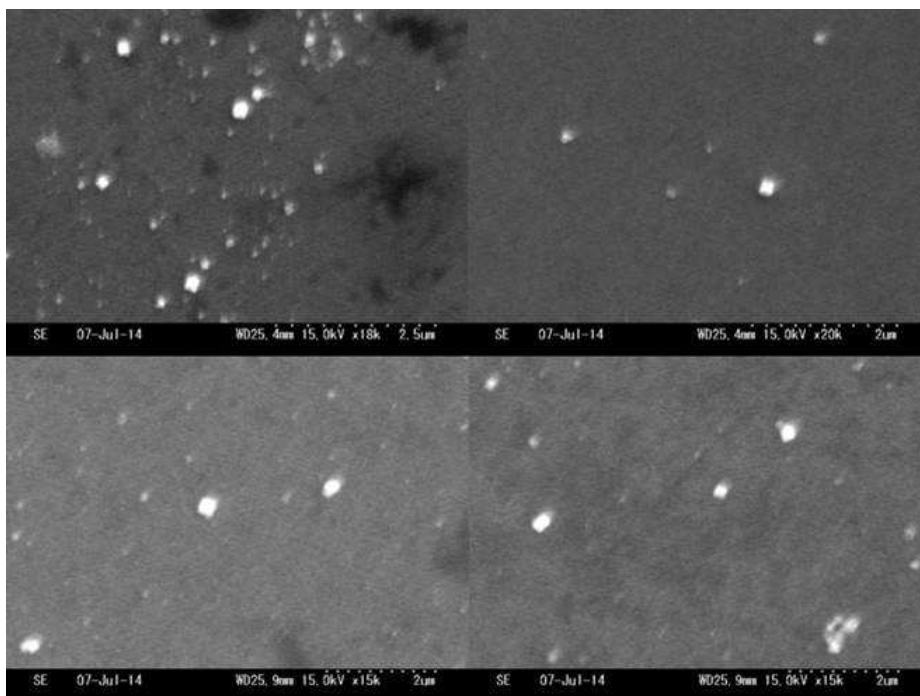


Figure 5.11 SEM image shows the formation of AgNPs. SEM images are taken after 10 min irradiation times while $[SHS] = 10 \times 10^{-3}$ M and $[AgNO_3] = 2 \times 10^{-4}$ M.

5.6 Hydrocarbon chain effect on AgNPs growth.

To confirm the effect of hydrocarbon chain on the NPs yield, we introduced different molecules which have same functional group but different carbon number such as SMS, SHS, SOS, SDS and AOT. When the numbers of carbon atoms were lower than 10 in the carbon chain; the additives did not affect so much on the growth of NPs as discussed the effect of SMS, SHS and SOS in detail. On the basis of

previous results with different additives, it was concluded that hydrocarbon chain is an important factor which effects on product yield. The growth process of Nps was supported by a molecules having long carbon chain (>10). As in the case of SDS and AOT, the CGC above which NPs would start to grow was observed. It was also confirmed that molecules having lower number of carbon atoms (<10) did not have CGC but have little effect on the product yield.

5.7 Effect of bis(p-sulfonate phenyl) phenyl phosphine dipotassium (BPPD)

5.7.1 Optical properties and SEM analysis

Figure 5.12 shows the absorption spectra after ns laser irradiation (300 mJ/cm^2). Initially the absorption peak appeared at 430 nm and the absorption increased without any shift till 45 min irradiation. It means that thermal effect is negligibly small and melting process does not occur; however, after longer irradiation time (60 min) the absorption peak start to shift towards the shorter wavelength (blue shift). Finally the peak observed at 396 nm after 135 min irradiation time. This peak position (396 nm) is same as we observed in case of AOT. We can conclude that using this method the individual role of each additive could be discussed.

Figure 5.13 shows the SEM images of the products obtained in BPPD- AgNO_3 solution after various irradiation times. After 120 min irradiation, the

absorption peak was observed at 400 nm and can be comparable with the results observed in case of SDS solution. SEM images also show that small nanoparticles were obtained. From the absorption spectra, the particle size would be 14 nm. After 30 min irradiation, cubic shaped NPs having rounded corners along with round shape of particles was obtained. Variety of NPs was obtained after 15 min irradiation which had sharp corners.

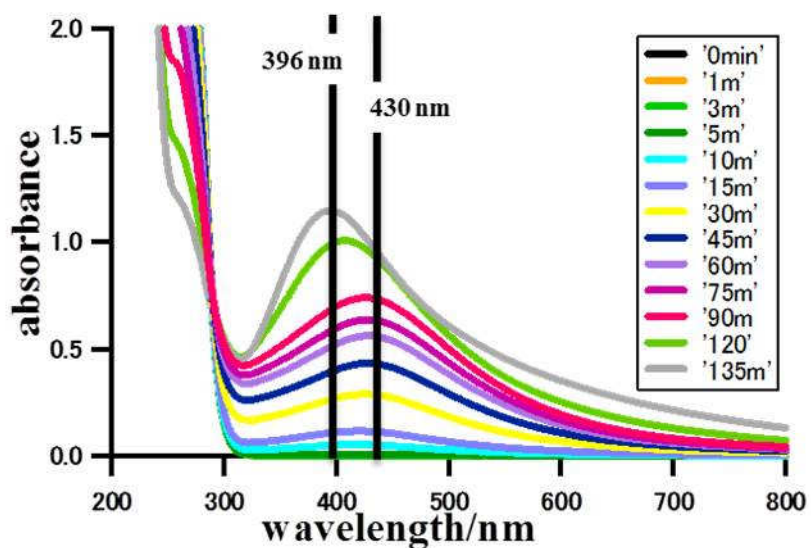


Figure 5.12 Absorbance spectra showing nanoparticle growth at $[BPPD] = 2 \times 10^{-4} \text{ M}$;

$[\text{silver nitrate}] = 2 \times 10^{-4} \text{ M}$.

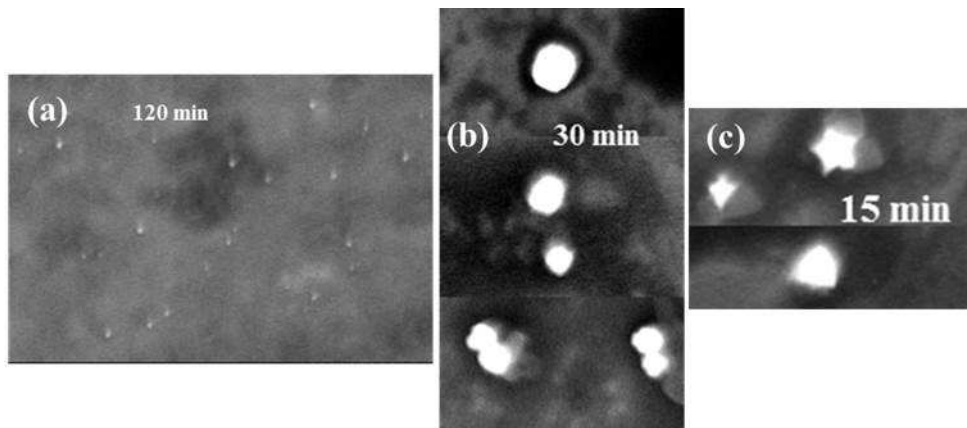


Figure 5.13 SEM images after ns laser irradiation: (a) 120 min; (b) 30 min; (c) 15 min

5.8 Conclusion

In this study, we investigated the effect of different additives on the formation process of AgNPs. These results open a new horizon to understand the shape controlling part of the reaction and concluded that different additives plays an important role in controlling the shape as well as the size of NPs (AOT and SDS results). Hydrocarbon chain also effect on the growth process. We found that the hydrocarbon chain <10 carbon atoms (SMS, SHS, SOS) did not show the CGC and had a little effect on the growth process. However; hydrocarbon chain > 10 carbon atoms (AOT, SDS) showed the CGC. This was the lowest limit at which the NPs would start to grow. Bigger molecules also control the size and shape of the product. According to the best of our knowledge, this is the first time to discuss the potential effect of each additive directly using light as reducing agent.

5.9 References

- [1] A. Tao, P. Sinsersuksakul, P. Yang, *Angew. Chem. Int. Ed.* **2006**, *45*, 4597.
- [2] T. Teranishi, M. Hosoe, T. Tanaka, M. Miyake, *J. Phys. Chem.* **1999**, *103*, 3818.
- [3] X. Wu, P. L. Redmond, H. Liu, Y. Chen, M. Steigerwald, L. Brus, *J. Am. Chem. Soc.* **2008**, *130*, 9500.
- [4] J. P. Camden, J. A. Dieringer, Y. Wang, D. J. Masiello, L. D. Marks, G.C. Schatz, R. P. V. Duyne, *J. Am. Chem. Soc.* **2008**, *130*, 12616.
- [5] Z. S. Pillai, P. V. Kamat, *J. Phys. Chem. B* **2004**, *108*, 945.
- [6] Q. Zhang, W. Li, L. P. Wen, J. Chen, Y. Xia, *Chem.—Eur. J.* **2010**, *132*, 11372.
- [7] C. Yee, M. Scotti, A. Ulman, H. White, M. Rafailovich, J. Sokolov, *Langmuir* **1999**, *15*, 4313.
- [8] Y. Sun, Y. Xia, *Science* **2002**, *298*, 2176.
- [9] K. Korte, S. E. Skrabalak, Y. Xia, *J. Mater. Chem.* **2008**, *18*, 437.
- [10] P. C. Lee, D. Meisel, *J. Phys. Chem.* **1982**, *86*, 339.
- [11] A. L. Koh, K. Bao, I. Khan, W. E. Smith, G. Kothleitner, P. Nordlander, S. A. Maier, D. W. McComb, *ACS Nano* **2009**, *3*, 3015.
- [12] R. Zana, J. Lang, C. Tondre, *J. Phys. Chem.* **1976**, *80*, 905.
- [13] M. R. Langille, M. L. Personick, C. A. Mirkin, *Angew. Chem. Int. Ed.* **2013**, *52*,

13910.

[14] K. Murakoshi, Y. Nakato in *Metal Nanostructures Synthesized by Photoexcitation* (Eds.: J. A. Schwarz, C. Contescu, K. Putyera), Marcel Dekker, New York, **2004**.

[15] M. Sakamoto, M. Fujistuka, T. Majima, *J. Photochem. Photobiol.C* **2009**, *10*, 33.

[16] M. Sakamoto, T. Majima, *Bull. Chem. Soc. Jpn.* **2010**, *83*, 1133.

[17] Q. Chen, X. Shen, H. Gao, *Adv. Colloid Interface Sci.* **2010**, *159*, 32.

[18] K. G. Stamplecoskie, J. C. Scaiano, *Photochem. Photobiol.* **2012**, *88*, 762.

[19] Yu. F. Zuev, R. Kh. Kurbanov, B. Z. Idiyatullin, O. G. Us'yarov, *Colloid J.* **2007**, *69*, 444.

[20] B. Z. Idiyatullin, K. S. Potarikina, Yu. F. Zuev, O. S. Zueva, O. G. Us'yarov, *Colloid J.* **2013**, *75*, 532.

[21] M. P. Pileni, *Nature Materials* **2003**, *2*, 145.

[22] D. F. Evans, D. J. Mitchell, B. W. Ninham, *J. Phys. Chem.* **1986**, *90*, 2817.

[23] M. P. Pileni, (ed.) *Reverse micelles* (Elsevier, Amsterdam, **1989**).

[24] M. P. Pileni, T. Zemb, C. Petit, *Chem. Phys. Lett.* **1985**, *118*, 414.

[25] J. Zeng, Y. Zheng, M. Rycenga, J. Tao, Z.Y. Li, Q. Zhang, Y. Zhu, Y. Xia, *J. Am. Chem. Soc.* **2010**, *132*, 8552

[26] A. Lo´pez-Miranda, A. Lo´pez-Valdivieso, G. Viramontes-Gamboa, *J. Nanopart.*

Res. **2012**, *14*, 1101.

[27] A. Tao, P. Sinsersuksakul, P. Yang, *Angew. Chem. Int. Ed.* **2006**, *45*, 4597.

[28] P. Somasundaran, D. W. Fuerstenau, *J. Phys. Chem.* **1966**, *90*, 70.

[29] U. Y. Qazi, S. Kajimoto, H. Fukumura, *Chem. Lett.* (in print)

Chapter 6

Photochemical synthesis of silver nanoparticles using UV pulsed laser irradiation in aqueous solution of silver acetate: effect of stabilizing agents

6.1 Introduction

Surfactant supported stabilization of the nanoparticles in aqueous solution has been demonstrated to be one of the most effectual method. Previous experimental studies elucidate that silver nanoparticles stabilized due to the presence of anionic surfactant i.e. sodium dodecyl sulfate (SDS) [1-2]. Chen et al. [3] obtained silver nanodisks from truncated triangular silver nanoplates at 40° C in the presence of hexadecyl trimethyl ammonium bromide (CTAB).

In this chapter, I describe the results of the preparation of nano sized Ag particles using 355 nm pulsed laser irradiation on aqueous solution of silver acetate as discussed in experimental section. Silver nitrate precursor is replaced with silver acetate. The effect of surfactants along with irradiation time on AgNPs size distribution and production efficiency was investigated. The whole process was carried out in an aqueous environment which is non-toxic, environment friendly and leading to a constant productivity in short reaction time (5 to 30 min) from the view point of mass production of material for industrial use.

6.2 Results and discussion

6.2.1 Optical properties

The optical properties of metal NPs are highly dependent on their size and shape

and show different colors due to resonant light scattering. After irradiating a sample solution with ns pulsed laser, a clear color change was observed. Figure 6.1 is pictures

of

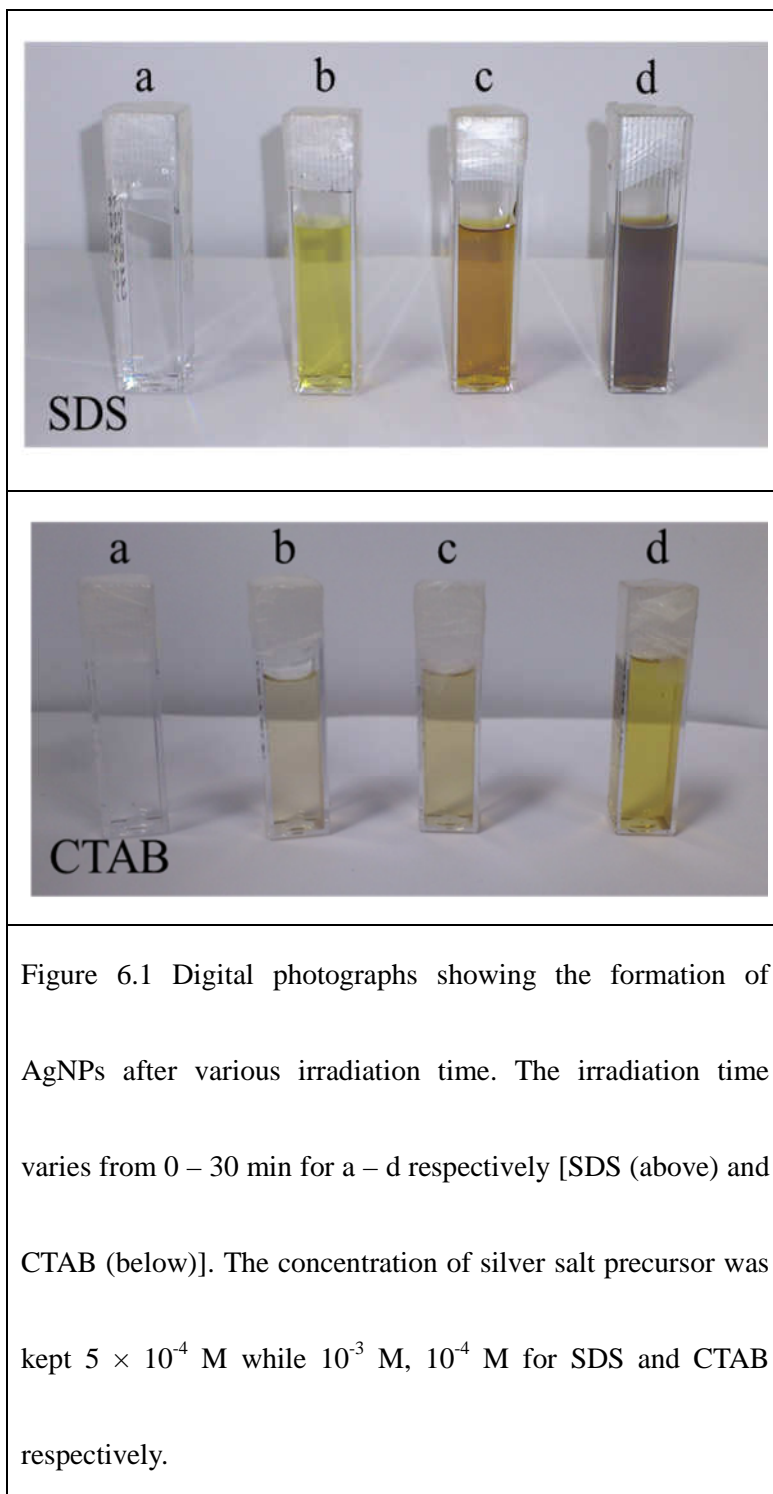
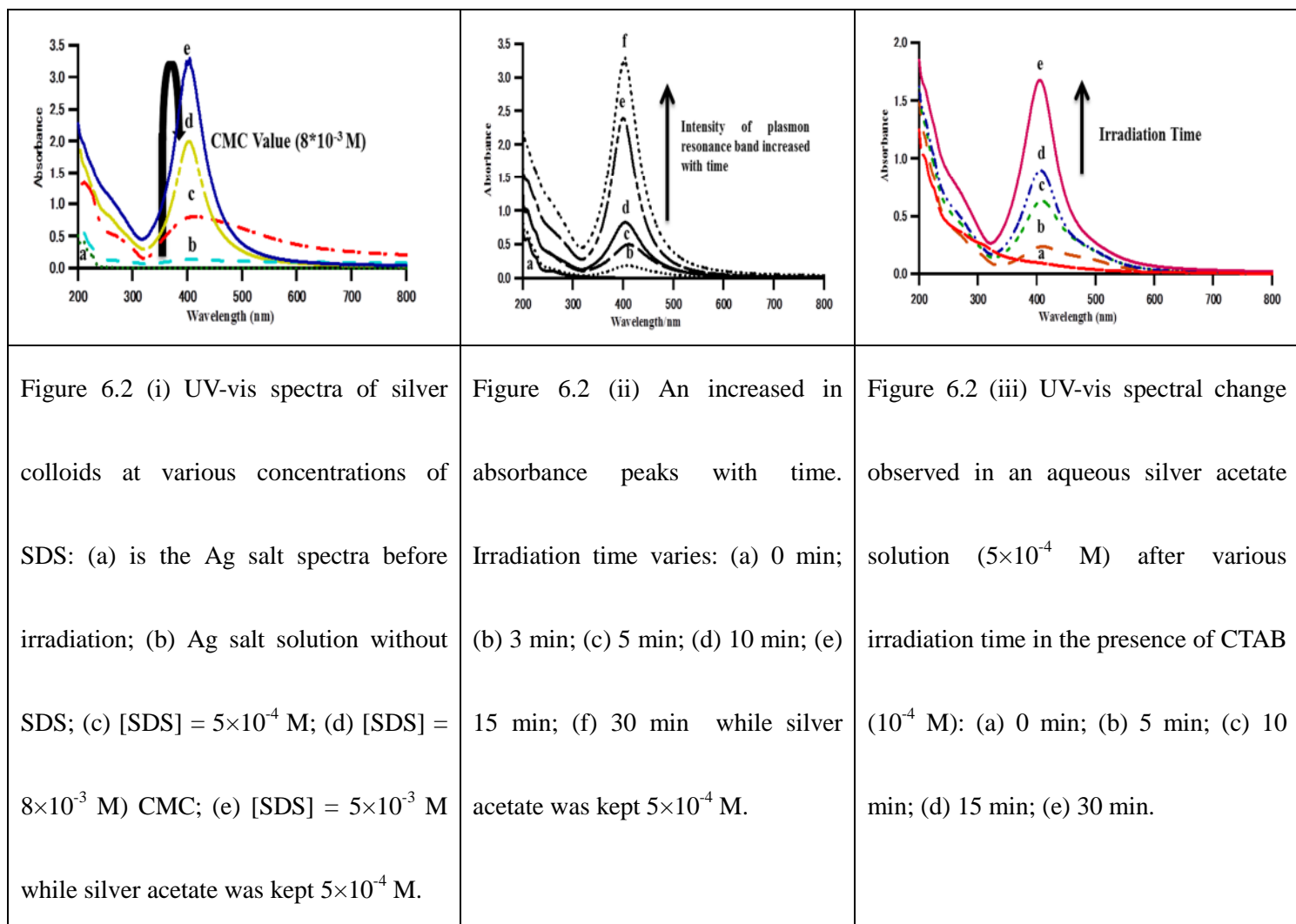


Figure 6.1 Digital photographs showing the formation of AgNPs after various irradiation time. The irradiation time varies from 0 – 30 min for a – d respectively [SDS (above) and CTAB (below)]. The concentration of silver salt precursor was kept 5×10^{-4} M while 10^{-3} M, 10^{-4} M for SDS and CTAB respectively.

photochemically reduced samples obtained after various times and conditions. After laser irradiation, the colourless silver acetate sample solution containing SDS and CTAB turned pale yellow to brown and light brown to pale yellow respectively. In case if we do not use any surfactant the optically transparent sample solution also turned to pale yellow colour after irradiation [4-5]. This result implies that AgNPs are formed inside the solution which may have different size of products.

Figure 6.2 shows the UV-visible absorption spectra of colloidal solutions obtained by laser irradiation in an aqueous solution of silver acetate ($5 \times 10^{-4} \text{M}$) and stabilizing agents (SDS, CTAB) at various time (0 ~ 30 min). The surface plasmon peak (SPR) after UV laser irradiation is appeared at 408 nm which indicate the formation of AgNPs while keeping all parameters constant, only by extending the irradiation time up to 30 min, the absorption intensity of the plasmon band was increased; however, the spectral shapes of the plasmon bands were nearly identical among those colloidal solutions. Figure 6.2 (i) shows UV-vis spectra of silver colloids prepared by ns UV laser (355 nm) irradiation (30 min) of an aqueous solution of silver acetate ($5 \times 10^{-4} \text{M}$) at various concentrations of SDS: (a) is the Ag salt spectra before irradiation; (b) Ag salt solution without SDS; (c) SDS ($5 \times 10^{-4} \text{M}$); (d) SDS ($8 \times 10^{-3} \text{M}$) critical micelle concentration value; (e) SDS ($5 \times 10^{-3} \text{M}$). Figure 6.2 (ii) shows an increased in



absorbance peak with time. The sample solution was prepared by dissolving silver acetate (5×10^{-4} M) in the presence of SDS (5×10^{-3} M). Irradiation time varies: (a) 0 min; (b) 3 min; (c) 5 min; (d) 10 min; (e) 15 min; (f) 30 min. Figure 6. 2 (iii) indicates the absorption spectra at various irradiation times in the presence of CTAB (10^{-4} M). This UV-vis spectral change observed in an aqueous silver acetate solution (5×10^{-4} M) after various irradiation time: (a) 0 min; (b) 5 min; (c) 10 min; (d) 15 min; (e) 30 min. The concentration of silver acetate was kept at 5×10^{-4} M, while the surfactants (SDS,

CTAB) amount was varied.

The increase in the absorbance of plasmon band implies that the number of NPs increased with time. As shown in Figure 6.3, the number of products increased from 0 to 5 mM of SDS concentration at the same irradiation time; (30 min) however, it decreased at its CMC value (8×10^{-3} M). Small amount of photochemically reduced Ag colloidal solution was taken to measure the size and shape on a SEM.

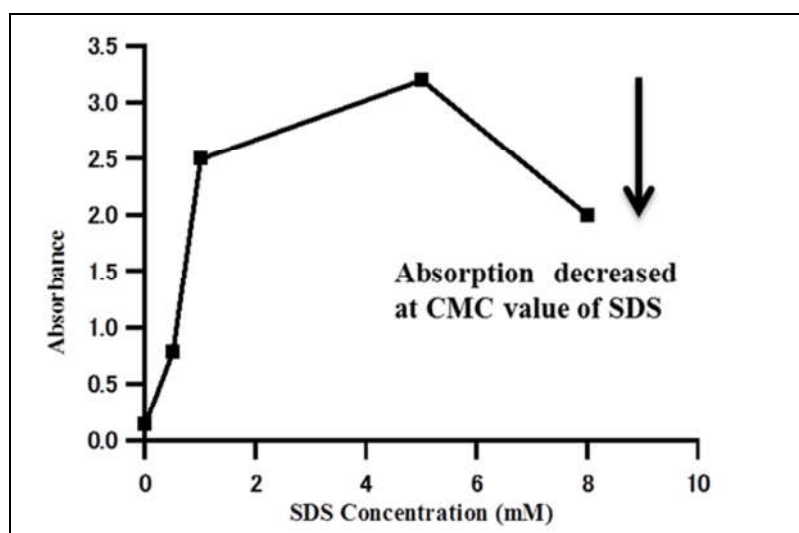
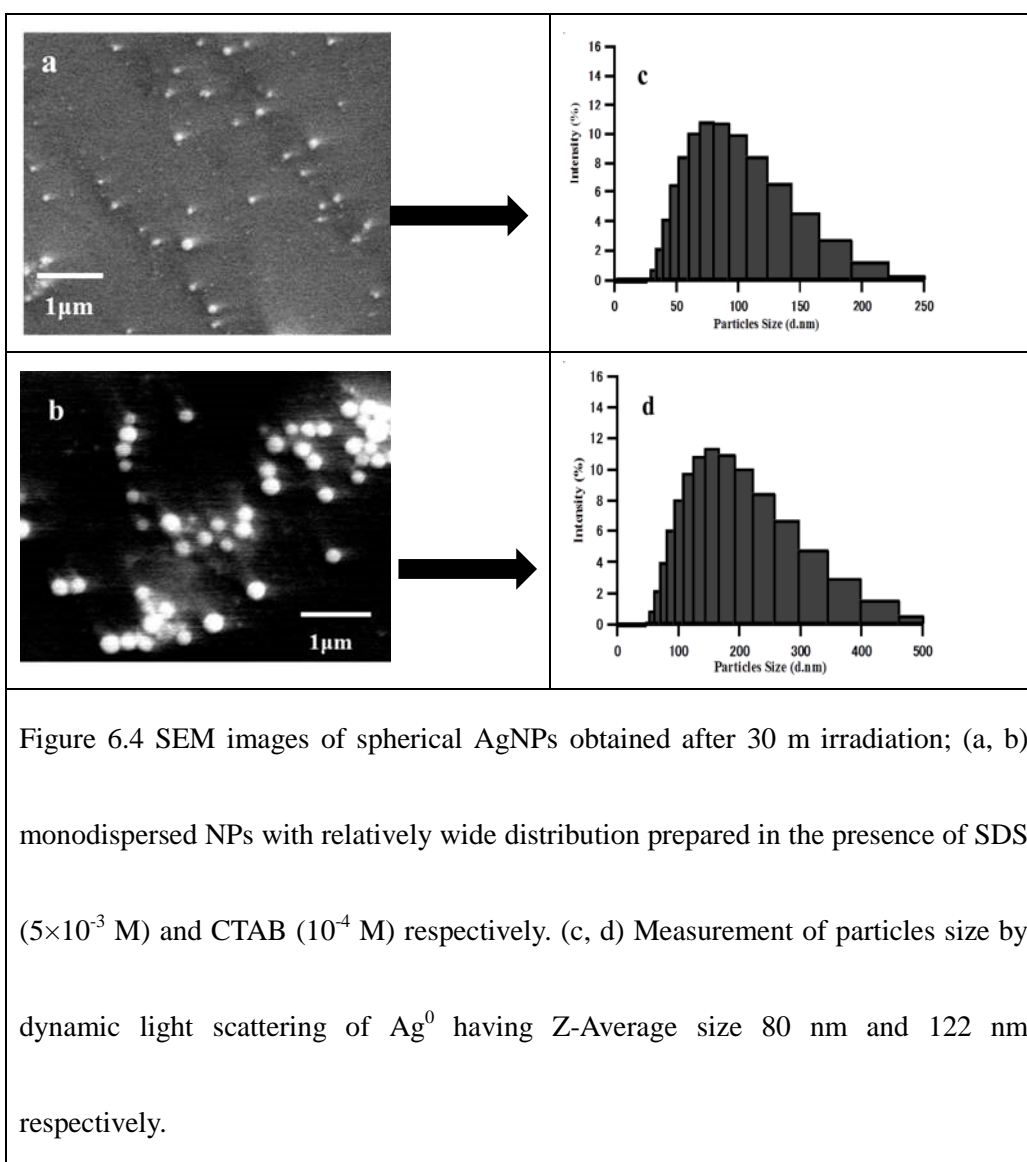


Figure 6.3 The change in the photo- reduction efficiency as a function of SDS concentration. Absorption peak decreased as the SDS concentration reached its critical micelle concentration value (8×10^{-3} M). [silver acetate] = 5×10^{-4} M.

6.2.2 Size, morphology and chemical composition

To gain further knowledge about the features of AgNPs obtained, analysis of the prepared samples on Indium Titanium Dioxide (ITO) glass were performed using SEM and EDX. The morphology and size of the particles were determined by SEM images and DLS. Figure.6.5 shows the SEM images of AgNPs prepared with various



SDS and CTAB concentrations after laser irradiation (30 min).

AgNPs were formed as a result of photoreduction of Ag^+ via biphotonic reaction as described in the previous chapter and stabilizing agents (SDS, CTAB) present in a sample solution can be adsorbed on the surface of synthesized NPs that prevent their aggregation. SEM images in Figure 6.4 show the formation of spherical shape AgNPs. The number of particles increased remarkably with 5 mM SDS solution compared to the lower concentrations solutions after 30 min irradiation time. On the other hand, large size spherical particle were observed in neat water. Furthermore, we kept safe our prepared samples and noticed that the color remains constant which shows the stabilization of silver colloidal solution. As discussed in chapter 3, aqueous solution of silver nitrate without using surfactants produce variety of products among them cubic shape nanoparticles were prominent; however, only spherical shape AgNPs were obtained which have different sizes. This is only due to the difference in silver salt precursor.

To obtain quick results of photoreduced product in terms of size distribution, DLS measurements were performed. The statistical size distribution graph versus intensity has been shown in Figure 6.4 (c-d). Particles were mono-dispersed with most of the particles size 80 nm, and 121 nm, prepared with high concentration of SDS (5×10^{-3} M)

and CTAB (10^{-4} M) respectively. We compared our results obtained with SEM to the ones obtained with DLS and found to be consistent however, in some cases slightly differ with SEM results. Slightly large size obtained by DLS is due to the fact that the measured sizes also contain the SDS and CTAB shell enveloping the core of AgNPs and the formation of aggregation [6]. However, an exact size distribution measurement is possible in a better way through SEM which has been used extensively for nanomaterial characterization.

The elemental analysis was performed using EDX on the SEM. Figure 6.5 shows the EDX spectrum of AgNPs prepared with this direct ns laser irradiation method. The presence of a band in the EDX spectrum is confirmation of the silver metal atoms. The results indicated that the reaction product was composed of high purity AgNPs. Similar results were obtained for each sample.

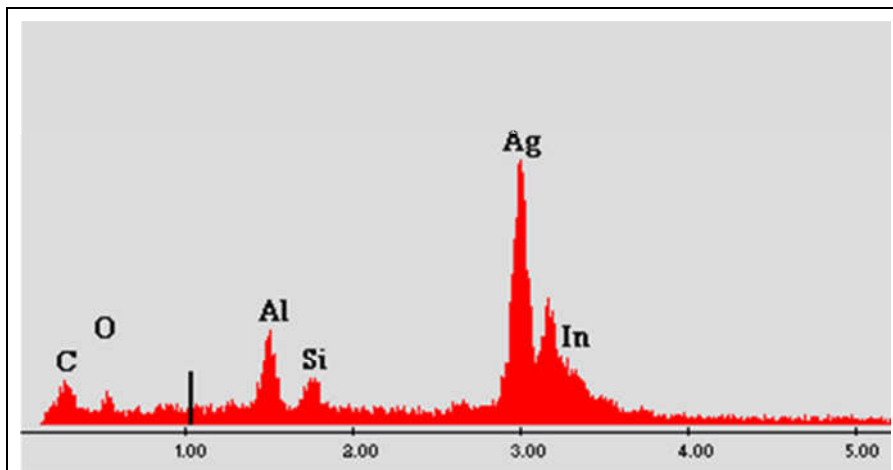


Figure 6.5 EDX spectrum of prepared silver nanoparticles. Other elemental peaks observed as the prepared sample was dried on Ito glass (Indium Titanium Oxide).

6.3 Conclusion

A critical need in the field of nano-science is the development of reliable, environmental friendly processes for fabrication of metallic NPs. In this study, we have successfully fabricated spherical AgNPs using UV pulsed laser (355 nm) irradiation in an aqueous solution of silver salt solution containing SDS and CTAB. The prepared Ag colloidal solution was stable enough to keep for a long time as it persist color for long time. The effects of stabilizing agents were investigated by

checking the morphology and size distribution of synthesized NPs. Mono-dispersed spherical silver particles had an average diameter 80 nm, 121 nm for SDS and CTAB respectively.

6.4 References

- [1] W. Que, Y. Zhou, Y. L. Lam, Y. C. Chan, C. H. Kam, *Appl. Phys. Lett.* **1998**, *73*, 2727.
- [2] I. Chakraborty, D. Mitra, S.P. Moulik, *J. Nanopart. Res.* **2005**, *7*, 227.
- [3] S. H. Chen, Z.Y. Fan, D. L. Carroll, *J. Phys. Chem. B* **2002**, *106*, 10777.
- [4] Y. S. Jae, S. K. Beom, *Bioprocess Biosyst. Eng.* **2009**, *32*, 79.
- [5] A. Henglein, *J. Phys. Chem. B* **1993**, *97*, 5457.
- [6] X. Li, J. J. Lenhart, H. W. Walker. *Langmuir* **2011**, *28*, 1095.

Chapter 7

Summary and conclusion

7.1 Summary and conclusion

Working on nanomaterials has been a hot topic for researches. It has been a crucial interest for researcher to develop an environmental friendly and simple route to synthesize them. In this study, we synthesized silver nanoparticles using ns laser light and discussed the effect of additives on synthesized photo-product.

In chapter 1, general aspects, various methods along with additives are overviewed and then the objective of the thesis is described. In chapter 2, experimental procedure and characteristic techniques are discussed in detail.

In chapter 3, I attempted to fabricate silver nanoparticles without using additives and observed the effect of laser irradiation time and intensity on the photo-product. Silver nanocubes were fabricated and discussed the growth process in detail. Log-log plot results gave an idea, initially the process was biphotonic and later turns into single photon; however, it was complicated to explain well. The comparison between CW and UV pulsed light confirmed that silver nanocubes increased their size by single photon absorption of photo-product present in the solution.

In chapter 4, silver nanoparticles were fabricated in the presence of SDS and discussed the concentration effect on nanoparticles. Silver nanospheres were fabricated successfully which had 14 nm sizes. Various concentrations of SDS were

used to discuss the effect on growth process. It was noticed that there is a lowest limit of SDS above that nanoparticles start to grow significantly. We call this lowest limit of SDS concentration as a critical growing concentration (CGC). It should be explained with the interaction between silver NS surfaces and SDS molecules as already pointed out that SDS molecules form two-dimensional aggregates (hemi-micelles) at a water and alumina interface even with a low SDS concentration.

In chapter 5, I attempted to know the individual role of each additive. It was noticed that hydrocarbon chains of molecules play an important role in growth process. Long chain hydrocarbon molecules are more effective to fabricate small sized nanoparticles; whereas small chain hydrocarbon molecules showed the opposite results. It was also confirmed that molecules with more than 10 hydrocarbon chain had CGC. This method clearly revealed the role of additives as light solely worked as a reducing agent.

In chapter 6, I attempted to change the silver salt precursor with silver acetate and discussed the effects of stabilizing agents CTAB and SDS in terms of their morphology and size distribution. It was observed that mono-dispersed silver particles had an average size diameter of spheres was 80 nm, 121 nm for SDS and CTAB, respectively.

ACKNOWLEDGEMENTS

In the name of Allah, the most gracious, the most merciful

Allah Who has made me energetic enough to accomplish this task with enough concentration and devotion, and finally blessed me with success. I cannot thank Him enough. All of my devotions and tributes to His Holy Prophet Muhammad (Peace and Blessing of Allah be Upon Him) Whose teaching enabled us to recognize our Creator.

This brief note should be considered as receipt to the compassion of the one whom I am indebted to for helping me during my research. The weightiest personality that comes to my mind is that of respected Prof. Hiroshi Fukumura my supervisor, whose guidance is blessing indeed for me. Personally, I have learnt a lot from him and I express my deepest gratitude for his painstaking efforts to improve my research skills and facilitating me in every possible way. Prof. Fukumura is someone you will instantly love and never forget once you meet him. He's very jolly and one of the smartest people I know. I hope that I could be as lively, enthusiastic, and energetic as Prof. Fukumura and to someday be able to command an audience as well as he can.

I am thankful to my co-supervisor Asst. Prof. Kajimoto-San who has been supportive and given me the freedom to pursue various projects without objection. He also provided insightful discussions about the research. I am also thankful to Prof. Shibata for his moral support and guidance in a right way.

In my lab-mates, I am very grateful to Ali Ahmad Ibrahim from Egypt for his scientific advice, knowledge and many insightful discussions and suggestions. He is my primary resource for getting my science questions answered. I am also very thankful to Hamza Alkindi from Oman for creating funny moments and cannot forget

the moments when he brings pizzas for me during night time stay for experiments.

I especially thank to my mom, sister and brothers. My hard-working parents have sacrificed their lives for kids and provided unconditional love and care. I love them so much, and I would not have made it this without them.

In the past hard time, I found my wife as a best friend and soul-mate. Rahat is the only person who can appreciate my quiriness and sense of humor. There are no words to convey how much I love her. She has been a true and great supporter and has unconditionally loved me during my good and bad times. She has been non-judgmental of me and instrumental in installing confidence. She has faith in me and my intellect even when I felt like digging hole and crawling into one because of no faith in myself. I truly thank to Rahat for sticking by my side, even when I was irritable and depressed. I feel that what we both learned a lot about life and strengthened our commitment and determination to each other and to live life to the fullest. I am thankful for her patience; allow me to concentrate fully on my research work.

I love my kids and thank to my daughter Aroosh and my son Muhammad Ahmad for their innocent smiles. They always made me happy and relaxed by creating funny moments. I welcome to my cute and sweet daughter Areej as a new addition in my family. She brings great blessing from Allah and I achieved many things which seem to be difficult.

At the end, I would like to thank Watanuki Foundation, Japan for their partial support of my PhD studies.

Umair Yaqub Qazi

*I dedicate this thesis to my
kids, Aroosh, Muhammad Ahmad and especially to my cute little angel Areej Umair*

I love you all dearly